JOURNAL OF GEOPHYSICAL RESEARCH, VOL. 99, NO. D3, PAGES 5263–5283, MARCH 20, 1994

Methodology for the estimation of terrestrial net primary production from remotely sensed data

A. Ruimy and B. Saugier

Laboratoire d'Ecologie Végétale, Université Paris-Sud, Orsay, France

G. Dedieu

Laboratoire d'Etudes et de Recherches en Télédétection Spatiale, Toulouse, France

Abstract. Kumar and Monteith's (1981) model for the remote sensing of crop growth has been used to estimate continental net primary productivity (NPP) as well as its seasonal and spatial variations. The model assumes a decomposition of NPP into independent parameters such as incident solar radiation (S_0), radiation absorption efficiency by canopies (f), and conversion efficiency of absorbed radiation into organic dry matter (e). The precision on some of the input parameters has been improved, compared to previous uses of this model at a global scale: remote sensing data used to derive f have been calibrated, corrected of some atmospheric effects, and filtered; e has been considered as biome-dependent and derived from literature data. The resulting global NPP (approximatively 60 Gt_C per year) is within the range of values given in the literature. However, mean NPP estimates per biome do not agree with the literature (in particular, the estimation for tropical rain forests NPP is much lower and for cultivations much higher than field estimates), which results in zonal and seasonal variations of continental NPP giving more weight to the temperate northern hemisphere than to the equatorial zone.

1. Introduction

Terrestrial net primary productivity (NPP) is the rate of atmospheric carbon uptake by vegetation through the process of net photosynthesis minus dark respiration. It is estimated at about 60×10^9 metric tons of carbon (Gt_C) per year for the whole of the continental surfaces, with rather large discrepancies between the estimates. For example, *Lieth*'s [1975] estimate is 53 Gt_C, while the *Ajtay et al.* [1979], *Fung et al.* [1987] and *Box* [1988] estimates are 58 Gt_C, 48 Gt_C and 68 Gt_C, respectively. Estimating NPP more precisely is important to understand the global carbon cycle: it is the greatest annual carbon flux from the atmosphere to the biosphere, and it is considered to be the main cause of the seasonal fluctuations in atmospheric CO_2 concentration [*Fung*, 1986]. The balance between NPP and respiration rate by nonphotosynthetic organisms (net ecosystem productivity (NEP)) determines whether there is accumulation of some of the excess atmospheric carbon by the biosphere, as assumed with indirect proofs: *Tans et al.* [1990] deduced from scenarios on CO_2 absorption by the oceans that to fit the observed atmospheric variations of CO_2 concentration, the land biosphere should also be a sink for CO_2, this sink being located in the northern hemisphere.

To estimate terrestrial NPP, two methods are available: (1) extrapolating field measurements for local NPP to the biosphere, using a vegetation map and (2) modelling plant productivity at the biosphere level. There are three main types of productivity models: (1) statistical models; *Lieth* [1975] presents various models correlating NPP to mean annual temperature, precipitation, and evapotranspiration respectively; (2) parametric models; *Kumar and Monteith* [1981] use the "efficiency" concept to decompose NPP into independent parameters such as incoming solar radiation, radiation absorption efficiency, and conversion efficiency of absorbed radiation into organic dry matter; (3) process models; the Frankfurt biosphere model (FBM) [*Lüdeke et al.*, 1993], the Osnabrück biosphere model (OBM) [*Esser*, 1992], for instance, take into account the basic processes of photosynthetic assimilation, respiration, and assimilate allocation.

The most sophisticated models are process models, but they are not satisfactory at the present time for use on a global scale because of the lack of parameters for most of the world ecosystems. This implies that either arbitrary values have to be used for some parameters or that the model has to be calibrated. A parametric model is therefore a good compromise between simplicity and precision in the description of the processes. Moreover, with a knowledge of the parameter variations interval, it is possible to give an error bar on NPP estimates.

In this paper we present our parametric model for the estimation of the terrestrial biosphere NPP and its seasonal and geographic variations. This model is based on *Kumar and Monteith*'s [1981] model for remote sensing of crop growth. A similar approach has already been used for the estimation of the terrestrial biosphere NPP by *Heimann and Keeling* [1989], but we have improved the precision on some input parameters: the radiation absorption efficiency and the conversion efficiency. The absorption efficiency has been derived from remote sensing data that we have corrected for some atmospheric effects, and we have introduced a biome-dependent conversion efficiency. This improved model has been used to estimate annual terrestrial NPP as well as its zonal and seasonal variations. We have also estimated annual and seasonal NPP per biome. All outputs have been compared to the existing literature.

Paper number 93JD03221.
0148-0227/94/93JD-03221/$05.00

2. Model

The model is based on the approach of *Monteith* [1972, 1977] and *Kumar and Monteith* [1981]. It considers instantaneous NPP (called P in the formulae) as a fraction of the incoming solar energy stored into organic dry matter:

$$P(t) = e(t) \times f(t) \times S_0(t) \quad (1)$$

where t is the time and S_0 is the incoming photosynthetically active radiation (PAR); f is the fraction of incoming PAR absorbed by the canopy (so-called "absorption efficiency"). According to *Jarvis and Leverenz* [1983] the fraction of PAR absorbed by the canopy is determined by (1) the direction of incoming radiation, (2) the proportion of diffuse radiation in the global radiation and its hemispheric distribution, (3) the spectral properties of the optical elements (leaves) in the PAR, (4) the spatial distribution of these elements, and (5) the structure of the canopy (leaf area index, leaf angles).

The conversion efficiency, e, is the fraction of absorbed PAR converted into organic dry matter. According to *Monteith* [1977] and *Gosse et al.* [1986] the conversion efficiency, e, is a relatively conservative value among plant formations of the same metabolic type. It can, however, vary with phenological stage, climatic conditions such as incoming radiation, temperature, and water stress [*Jarvis and Leverenz*, 1983].

One must note that equation (1) has been validated in terms of annual production, i.e., integrated over a growing season, and mainly used for crops in temperate regions, where agricultural practices tend to limit water or nutrient stresses.

3. Data

The model described above has been used to estimate NPP on a global scale with a time step of 1 week on a regular 1°×1° grid (Plate Carrée projection). Conversion efficiency, e, has been derived from literature with respect to the vegetation class. Absorption efficiency, f, is estimated through the use of remotely sensed radiances, while the incoming PAR, S_0, is derived from climate model runs.

3.1. Incoming Photosynthetically Active Radiation, S_0

Global solar radiation at the surface is derived on a monthly basis from an output of a global climate model (GCM) of the French Meteorological Office [*Planton et al.*, 1991] and consists of climatology (perpetual January, February, etc). The original Gauss projection with a latitude-varying resolution of about 2.8° has been resampled to a regular 1°×1° grid. The fraction of PAR in the global radiation is assumed to be 0.48 [*McCree*, 1972]. According to *Szeicz* [1974] this fraction may vary from 0.45 to 0.53. It is well known that solar radiation calculation by GCMs is far from satisfactory and that satellite estimates may give better estimates [e.g., *Dedieu et al.*, 1987; *Whitlock et al.*, 1990]. Global data sets derived from the satellite based method will probably be available in the near future.

3.2. Absorption Efficiency, f

According to several works, f, the fraction of incoming PAR absorbed by the canopy can be related to various combinations of red (R) and near-infrared (NIR) surface reflectances of the canopy. To map this parameter, f, on a global scale with a high temporal resolution, we used radiometrically corrected satellite measurements.

3.2.1. Satellite data processing. Absorption efficiency estimates are based on the second generation of the global vegetation index (GVI) product provided by NOAA [*Tarpley et al.*, 1984]. We used the data for the year 1986. The product is available for the period April 1985 to December 1991, on a weekly basis, in the Plate Carrée projection with a resolution of 0.144°. It consists of a resampling of NOAA/AVHRR GAC data and contains raw digital counts in the red (R: 0.58 - 0.68 μm) and near-infrared (NIR: 0.73 - 1.1 μm) channels, calibrated measurements of two thermal infrared channels (10.2 - 11.3 and 11.5 - 12.5 μm) as well as scan angle, solar zenith angle, and NDVI calculated from raw digital counts. The value of each pixel in the various channels corresponds to the maximum vegetation index out of the seven values of a week, a method (the so-called maximum value composite (MVC) technique [*Holben*, 1986]) used to minimize the effect of high atmospheric optical depth (clouds, aerosols).

According to several works, f, the fraction of incoming PAR absorbed by the canopy can be linearly related to the normalized difference vegetation index (NDVI), defined as a combination of red (R) and near-infrared (NIR) surface reflectances of the canopy:

$$NDVI = \frac{\rho_{NIR} - \rho_R}{\rho_{NIR} + \rho_R} \quad (2)$$

where ρ_R, ρ_{NIR} are surface reflectances in the red and near-infrared wavelengths, respectively.

$$f = a + b \times \text{NDVI} \quad (3)$$

We use this linear relationship and NDVI to retrieve as precisely as possible the actual canopy absorption efficiency from remotely sensed reflectances. To do that we have calibrated raw data and taken into account atmospheric effects on the remote sensing measurements. The problem is then to determine the coefficients, a and b, of equation (3). Figure 1 represents

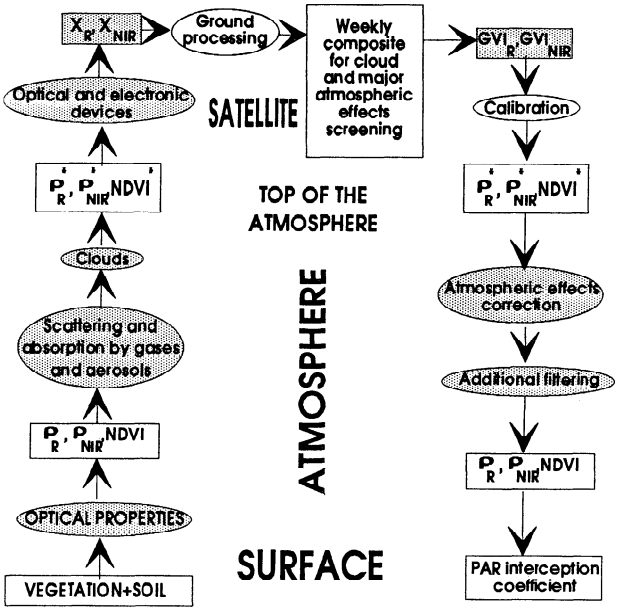

Figure 1. Model for the estimation of the fraction of photosynthetically active radiation (PAR) absorbed by the terrestrial vegetation (f) from remotely sensed data.

diagrammatically the various steps we have followed to retrieve f from the available data.

First, top of the atmosphere (TOA) reflectances, ρ^*, are calculated from GVI raw digital counts using calibration factors derived by *Holben et al.* [1990]:

$$\rho^* = \frac{\rho \times r^*}{E_s \times cos(\sigma_s)} \quad (4)$$

where r^*, radiance in the channel, is equal to $a \times (x - x_0)$; a is calibration coefficient; x_0 is offset; x is digital count for the channel; E_s is solar irradiance in the spectral band (seasonal Earth-Sun distance variation is taken into account); and σ_s is solar zenith angle. Then, atmospheric effects are taken into account. We used the SMAC method [*Rahman and Dedieu*, 1992], derived from the 5S code (satellite signal simulation in the solar spectrum) [*Tanré et al.*, 1990] to estimate surface reflectances, ρ [*Escartin*, 1990]. For this preliminary work, only Rayleigh scattering has been accounted for:

$$\rho^* = \rho_a + \frac{T(\sigma_s) \times T(\sigma_v) \times \rho}{1 - \rho \times a} \quad (5)$$

where $T(\sigma_s)$ is total scattering transmission on downward path; $T(\sigma_v)$, total scattering transmission on upward path; ρ_a, atmospheric reflectance; a, spherical albedo of the atmosphere.

Red and near-infrared surface reflectances are used to compute surface NDVI. While maximum NDVI calculated from raw counts is always below 0.45, our calibrated and atmospherically corrected NDVI reaches about 0.8. Radiative transfer calculation [e.g., *Sellers*, 1985] as well as ground experiment [e.g., *Asrar et al.*, 1984] show that surface NDVI can reach up to 0.9. The difference between our 0.8 maximum and this 0.9 value is probably due to absorption and scattering processes not taken into account by a simple Rayleigh scattering correction. The surface NDVI we obtained remains very scattered, mainly because of clouds and surface directional effects. In addition to the MVC technique already applied by NOAA, we further filtered the signal using the best index slope extraction (BISE) method [*Viovy et al.*, 1992]. This filter retains the upper envelope of the NDVI time series and sticks close to it during growth and decrease of the signal. Reflectances corresponding to the filtered points are resampled at a constant weekly interval. Red and near-infrared surface reflectances are then averaged over 1°×1° grid and then used to compute surface NDVI. This method is expected to retrieve a signal close to surface NDVI except in the following cases: (1) if too few unclouded days are found in the time series (like on equatorial rain forest pixels), the signal remains lower than surface NDVI; and (2) directional effects or artefacts in the measurement chain that produce a high signal are kept by the filter.

3.2.2. Relationship between surface NDVI and *f*. The assumption of a linear relationship between f and surface NDVI is based on results of experiments on cultivations and natural vegetation and on results of models of radiative transfer within canopies (Table 1).

Experimental results: For crops in the growing phase, both *Asrar et al.*[1984], *Hatfield et al.*[1984], *Baret and Olioso* [1989], and *Daughtry* [1988] find that a linear relationship is satisfactory with high linear correlation coefficients. The relationship is similar for the different authors. But *Gallo et al.* [1985] with corn field data find that a parabolic relationship is a better approximation. For *Kumar and Monteith* [1981], there is a linear relationship but between f and the simple ratio (SR) of near-infrared and red reflectances. In the senescent phase, the authors find linear relationships but with much different coefficients: in this phase, the canopy still intercepts the incoming radiation, but the leaves contain less photosynthetic pigments which leads to a decrease in NDVI. Only two experimental results were found for natural vegetation in the literature [*Bartlett et al.*, 1990; *Peterson and Running*, 1989]. While a linear relationship still applies, it is much different for these two types of natural vegetation (a grassland and a coniferous forest), the two being also significantly different from that for crops.

Model simulations: Various authors have also used models of radiative transfer within the canopy to correlate the outputs concerning NDVI and f for various input data sets (various optical properties of soil and leaves, canopy structure, etc.). For most input sets and varying leaf area indices, nonlinear relationships are found. However, when the outputs of a model run for several input sets are plotted on the same graph, relatively good linear correlation coefficients are found [*Baret and Olioso*, 1989; *Baret et al.*, 1989; *Leon*, 1991].

Both experiments on cultivated plots (in the growing phase) and radiative transfer models lead to the conclusion that a linear relationship between f and NDVI is realistic. These relationships present a conservative slope (between 1.2 and 1.3), but the intercept varies more (between -0.31 and -0.06), probably because of difference in the type of soils. However, to draw a conclusion on the validity of a linear, constant relationship between f and NDVI in all cases, there are numerous drawbacks: (1) there are too little data on natural vegetation types; (2) the only data set found on coniferous forest seems to indicate that the relationship is different than for broad-leaved forests; (3) for crops, linear relationships are found either between f and NDVI or between f and SR, which is in contradiction; (4) the theory predicts a nonlinear relationship with a shape varying with parameters such as the canopy structure, the soil type, etc. [*Leon*, 1991]. In any case, a linear relationship either between f and NDVI or f and SR is an approximation, and it is only valid for vegetation in the growing phase.

Empirical relationships: In this study as well as in *Loudjani*'s [1988], an empirical linear relationship between f and NDVI is assumed, the coefficients being determined with the following two points: no interception corresponds to NDVI on the desert, total interception corresponds to maximum NDVI on the equatorial forest. With NDVI computed from the raw digital counts, *Loudjani* [1988] found: f_i = -0.07 + 2.53 × NDVI (f_i, fraction of PAR intercepted).

With corrected and filtered satellite data we find a slope for equation (3) close to the experiment and model results, with an intercept close to 0:

$$f = -0.025 + 1.25 \times \text{NDVI} \quad (6)$$

This slope of 1.25 is about half the slope Loudjani found, the discrepancy being attributed to a difference of roughly a factor of 2 between NDVI calculated with raw counts and NDVI that is calibrated and atmospherically corrected.

In conclusion the NDVIs we derived from remote sensing data after calibration and atmospheric effects correction are expected to be closer to surface NDVI than are NDVIs computed from raw digital counts. At the surface a linear relationship between f and NDVI seems to be a good approximation to

Table 1. Relationships Found in the Literature Between the Fraction of Photosynthetically Active Radiation Absorbed (f) or Intercepted (f_i) by the Canopy and the Vegetation Index (NDVI or SR)

Vegetation Type or Model	Experimental Conditions	Relationship	Reference
	Experiment Results, Cultivations, Growing Phase		
Spring wheat United States	5 sowing dates, 4 irrigation rates	$f = -0.11 + 1.25 \times NDVI$	*Asrar et al.* [1984]
Spring wheat United States	5 sowing dates, 4 irrigation rates	$f = -0.18 + 1.20 \times NDVI$	*Hatfield et al.* 1984]
Corn, soybeans United States	various sowing dates, densities	$f = -0.14 + 1.28 \times NDVI$	*Daughtry* [1988]
Corn United States	various sowing dates, densities, 3 soils	$f = 0.6 - 2.2 \times NDVI + 2.9 \times NDVI^2$	*Gallo et al.* [1985]
Sugar beet Great Britain	3 sowing dates	$f_i = 0.125 \times SR$	*Kumar and Monteith* [1981]
Wheat Great Britain	3 sowing dates	$f_i = -0.69 + 0.31 \times SR$	*Kumar and Monteith* [1981]
Winter wheat France	2 varieties, various angles	$f = -0.06 + 1.23 \times NDVI$	*Baret and Olioso* [1989]
	Experiment Results, Cultivations, Senescent Phase		
Spring wheat United States	5 sowing dates, 4 irrigation rates	$f = 0.68 + 0.26 \times NDVI$	*Hatfield et al.* [1984]
Corn United States	various sowing dates, densities, 3 soils	$f = 0.56 + 0.40 \times NDVI$	*Gallo et al.* [1985]
	Experiment Results, Natural Vegetation		
Salt marsh United States	3 physiognomies, 2 fertilization types	$f_i = -0.37 + 1.39 \times NDVI$	*Bartlett et al.* [1990]
Conifers United States	3 localities	$f = -0.20 + 1.00 \times NDVI$	*Peterson and Running* [1989]*
	Model Simulations		
SAIL model	various input sets	$f = -0.31 + 1.33 \times NDVI$	*Baret and Olioso* [1989]
Simple model	various input sets	$f = -0.23 + 1.24 \times NDVI$	*Baret et al.* [1989]
Sellers model	various input sets	$f = -0.15 + 1.28 \times NDVI$	*Leon* [1991]

* NDVI calculated from leaf area index values, using equation (7).

estimate PAR interception. The greatest errors in using a constant linear f/NDVI relationship are expected in area with low NDVI, i.e., area with small vegetation cover. According to *Huete* [1989], errors caused by soil effects amount to about 10%. In this study, directional effects were not accounted for, even though they could significantly lower or increase the signal.

3.3. Conversion Efficiency of Absorbed Photosynthetically Active Radiation Into Organic Dry Matter, e

Dry matter production is the balance between photosynthetic gains and respiratory losses of a plant community over a period of time. Conversion efficiency e of absorbed radiation into dry matter can thus be decomposed into photosynthetic efficiency (ratio canopy net photosynthesis / radiation absorbed) and respiratory losses. Therefore environmental factors on which either photosynthetic, respiratory, or radiative processes depend can modify conversion efficiency. Some important identified factors are given.

Natural or cultivated vegetation: In temperate zones at least, cultivated vegetation types have much higher e, due to the choice of fast-growing species and the optimal conditions (irrigation and fertilization), all factors enhancing photosynthetic efficiency.

Woody or herbaceous vegetation: Woody plants have a lower e, due to the extra respiration costs of maintaining nonphotosynthetic organs (stems and roots).

Temperature: Maintenance respiration varies exponentially with temperature, whereas photosynthetic efficiency is little affected by temperatures in the normal range (5° - 30°C). Therefore e decreases as we go from boreal to equatorial latitudes with higher mean temperatures.

Water availability: Dry zone vegetation types have lower e than moist zones, due to the decrease in photosynthetic efficiency induced by water stress.

Metabolic type: Plants having a C_4 metabolism have a higher photosynthetic efficiency (and therefore conversion efficiency) than plants in C_3. Among C_3 plants, non legumes have a higher e than legumes due to the added cost of nitrogen fixation for the latter.

We do not presently have a parameterization of all these factors, but we ranged e according to the main vegetation types (ecosystem types being broadly correlated with a set of environmental conditions). Inside each vegetation type however we assumed e to be constant. Mean values for each biome are calculated from literature data, and global vegetation maps [*Matthews*, 1983; *Wilson and Henderson-Sellers*, 1985] are used to map the conversion efficiencies.

3.3.1. Literature research of conversion efficiencies into aboveground dry matter, e_a. We have searched for data on conversion efficiency defined as the ratio of aboveground NPP to absorbed or intercepted radiation during the growing season, since data on aboveground production are the most commonly available. These data were aboveground net primary production during a year (i.e., the algebraic sum of leaf production, wood increment, and sometimes flower and fruit production, mortality) and the sum of absorbed radiation during the growing season. The latter can be estimated with a model of light interception by

the canopy, for example, Monsi and Saeki's empirical formula [1953]:

$$f = a_{max} \times (1 - e^{-k \times L}) \quad (7)$$

where a_{max} is maximum absorption at full light interception (a_{max} = 0.95); L is leaf area index; and k is light extinction coefficient (k = 0.6 when no value could be found). (In the case of rain forests we have used values of annual NPP and incoming radiation, considering a constant value of $f = a_{max}$ = 0.95). All the resulting values for natural vegetation types and tree plantations found in the literature are shown in Table 2. For more complete compilations of existing values on herbaceous crops, see *Gosse et al.* [1986] and *Prince* [1991]. In general, there is a lack of values concerning natural vegetation types in the literature. Most of the values found concerned herbaceous crops and tree plantations. Among natural vegetation types, forest values are the most numerous. Grassland values are very scarce, in particular tropical grasslands values. Contrarily to *Monteith* [1977] we found a great intrabiome and interbiome heterogeneity. Even within a subclass, for instance C_3 herbaceous crops, values quoted by *Gosse et al.* [1986] range from 1.83 g MJ^{-1} for winter rapeseed to 3.50 for potato. The causes for this heterogeneity could be: experimental errors, differences in the methods used (e.g., radiation absorption result from measurements or modeling) or in the quantities measured (e.g., absorbed or intercepted radiation). On the other hand, conversion efficiencies may actually differ between species, or / and vary with certain environmental parameters.

Considering the lack of values for some classes and the variability of the values, the calculated means (Table 2) have to be considered with great care. General trends are however in accordance with our a priori knowledge: the mean efficiency is higher for crops than for natural vegetation, it is higher at high latitude than for equatorial forests; it is higher for equatorial rain forests than for Mediterranean or tropical dry forests, it is higher for natural grasslands than for tree formations of the same latitude. (We discarded the only value found for a mixed broad-leaved / coniferous forest: 0.55 g MJ^{-1} [*Whittaker and Woodwell*, 1969], as it is lower than means calculated on both pure broad-leaved and coniferous stands.)

3.3.2. Literature research of ratios belowground / aboveground net primary productivity, P_s/P_a. To estimate total NPP, we need to know the conversion efficiency of absorbed radiation into total dry matter (e). We have already assumed that conversion efficiency into aboveground dry matter (e_a) is constant within the major ecosystem types. We consider now that the ratio of belowground NPP to aboveground NPP (P_s/P_a) is a constant, and

$$e = e_a \times (1 + P_s/P_a) \quad (8)$$

A literature research has been done to estimate a mean P_s/P_a ratio for the biomes for which values of e_a were found (Table 3). Concerning forest ecosystems, most values result from the International Biological Program [*DeAngelis et al.*, 1981], and show P_s/P_a ratios usually low (about 0.2). However, the determination of belowground productivity of trees is very awkward, so productivity is usually estimated from the ratio of belowground to aboveground biomass, which underestimates fine root turnover. *Ågren et al.* [1979] have made more careful estimates to conclude that the ratio of 0.2 usually quoted is underestimated. Concerning grasslands, most values found are quoted by *Sims et al.* [1978] and are on the contrary surprisingly high (up to 6). Because the raw means lead to unrealistic values of conversion efficiency, we used an arbitrary value of 0.5. Annual ratios for herbaceous crops are usually more precisely estimated and are very low (about 0.1).

3.3.3. Mean conversion efficiencies of absorbed photosynthetically active radiation into total dry matter, e, and conversion efficiency mapping. To assign to each 1°×1° land pixel a value of e, we needed a list of e per vegetation type and a vegetation map. However, several problems arouse.

1. The two vegetation maps available [*Matthews*, 1983; *Wilson and Henderson-Sellers*, 1985] were not completely appropriate for our study, being not based on the criteria that seemed the most important in determining the value of conversion efficiencies, e (see above, the factors that influence e). So we reclassified the Matthews and the Wilson and Henderson-Sellers vegetation types with the criteria described above, i.e., natural or cultivated vegetation; woody or herbaceous formations, or respective fraction of the two; latitudinal band; moist or dry zone; for herbaceous formations, metabolic type (C_3/C_4). The original classes did not all fit in our system. For instance, all the Matthews classes are not based on the latitudinal criterion, so most shrubland and herbaceous formations are found under all latitudes. In this case we reclassified the original classes according to the latitudinal band where they are the most abundant. Table 4 recapitulates the new vegetation classes defined, and the correspondence to the Matthews and Wilson and Henderson-Sellers original classes.

2. Even with this simplified classification, we could not find in the literature a set of values of e for each vegetation type. Arbitrary values of e_a, P_s/P_a, or e had to be attributed to some classes. Table 5 shows the biome-dependent e finally used as inputs for our numerical experiments, these resulting either from the literature research or extrapolated with adequate hypotheses (values with an asterisk). The hypotheses are explained below, in description of reference experiment.

3. The 1°×1° land pixels are not all made of a single vegetation type. The two available maps present a different approach to take into account the heterogeneity of the pixels: Matthews vegetation and land use map [1983] gives for each pixel the potential, natural vegetation type, and the fraction of cultivated land (0, 20, 50, 75, or 100% cultivation). The conversion efficiency for a composite pixel (natural plus cultivated vegetation) is assumed in our study to be the mean of e for the natural vegetation type (defined by the vegetation map) and of e for cultivations, weighted by the cultivation fraction (defined by the land-use map). Wilson and Henderson-Sellers major and secondary vegetation map [1985] gives for each pixel the major (over 50% cover fraction) and the secondary (less than 50% cover fraction) vegetation types, these being either natural or cultivated. As we do not have more precise information on the fraction of the two types, for each pixel, the conversion efficiency is assumed to be e of the major vegetation type.

4. Numerical Experiments

Table 5 recapitulates the mean e per biomes, and Table 6 recapitulates the other inputs used in each experiment.

4.1. Reference Experiment, Experiment REF

The different hypotheses to extrapolate a value of e for the classes in which no literature value could be found are the

Table 2. Conversion Efficiencies of Absorbed PAR Into Aboveground Dry Matter and / or Total Dry Matter Found in the Literature, or Calculated Using Appropriate Data

Vegetation Type	Species	Age	Locality	Growing Season	R_0	S_i	P_a	L_{max}	e_a	e	References
EF	climax rain forest	mature	Malaisia	12 months	5440	2480	2290	8.0	0.92		*Kira* [1978]
	climax rain forest	mature	Ivory Coast	12 months	5680	2590	1630	8.3	0.63		*Bernhardt-Reversat et al.* [1978]
	climax rain forest	mature	Ivory Coast	12 months	6019	2744	1150	?	0.42		*Müller and Nielson* [1965]
	climax rain forest	mature	Puerto Rico	12 months	4227	1927	1033	?	0.53		*Jordan* [1971]
	secondary forest	0 - 1	Rio Negro valley	12 months	5200	2230	840	2.3	0.38	0.40	*Saldarriaga and Luxmoore* [1991]
	secondary forest	1 - 3	Rio Negro valley	12 months	5200	2590	1151	3.9	0.44	0.49	*Saldarriaga and Luxmoore* [1991]
	secondary forest	3 - 10	Rio Negro valley	12 months	5200	2650	1225	4.5	0.46	0.50	*Saldarriaga and Luxmoore* [1991]
	secondary forest	10 - 20	Rio Negro valley	12 months	5200	2720	656	6.0	0.24	0.26	*Saldarriaga and Luxmoore* [1991]
	secondary forest	20 - 35	Rio Negro valley	12 months	5200	2720	627	6.1	0.23	0.24	*Saldarriaga and Luxmoore* [1991]
	secondary forest	35 - 60	Rio Negro valley	12 months	5200	2720	684	6.2	0.25	0.27	*Saldarriaga and Luxmoore* [1991]
	secondary forest	60 - 80	Rio Negro valley	12 months	5200	2720	589	6.3	0.22	0.22	*Saldarriaga and Luxmoore* [1991]
	secondary forest	80 - 200	Rio Negro valley	12 months	5200	2730	701	6.7	0.26	0.26	*Saldarriaga and Luxmoore* [1991]
Mean									0.56		
MF	evergreen oak	?	France	?	5400	2432	650	4.4	0.34		*Eckardt et al.* [1975]
	evergreen forest (hypothetic)	?	warm-temperate	?	3000	?	460		0.30		*Jarvis and Leverenz* [1983]
Mean									0.32		
TF+AF	oak-pine	40	New York	?	?	?	857	3.8	0.55		*Whittaker and Woodwell* [1969]
TF	chestnut coppice	11	France	01.05/10.11	4053	931	1236	3.6	1.33		*Sabatier-Tarrago* [1989]
	chestnut coppice	26	France	01.05/10.11	4053	1015	1182	4.7	1.16		*Sabatier-Tarrago* [1989]
	chestnut coppice	26	France	01.05/10.11	4053	940	1161	3.7	1.23		*Sabatier-Tarrago* [1989]
	chestnut coppice	44	France	01.05/10.11	4053	1003	917	4.5	0.91		*Sabatier-Tarrago* [1989]
	chestnut coppice	41	France	01.05/10.11	4053	1002	1069	4.5	1.07		*Sabatier-Tarrago* [1989]
	chestnut coppice	46	France	01.05/10.11	4053	1009	947	4.6	0.94		*Sabatier-Tarrago* [1989]
	oak-hickory	various	Tennessee	01.04/12.12	4100	1452	775	4.9	0.53		*Baldocchi et al.* [1987], *DeAngelis et al.* [1981]
	oak	20	U.S.S.R.	?	?	?	?	?	0.86		*Rauner* [1976]
	oak	40	U.S.S.R.	?	?	?	?	?	0.80		*Rauner* [1976]
	oak	80	U.S.S.R.	?	?	?	?	?	0.46		*Rauner* [1976]
	oak	120	U.S.S.R.	?	?	?	?	?	0.40		*Rauner* [1976]
	oak	160	U.S.S.R.	?	?	?	?	?	0.34		*Rauner* [1976]
	oak	200	U.S.S.R.	?	?	?	?	?	0.23		*Rauner* [1976]
	oak	80	Belgium	08.05/13.11	3911	967	1224	6.8	1.26		*Galoux et al.*[1981], *DeAngelis et al.* [1981]
	beech forest	mature	France	22.04/10.11	4053	1155	871	6.6	0.75		*Lemée* [1978]
	beech sapling	young	France	22.04/10.11	4053	1155	763	6.6	0.66		*Lemée* [1978]
	deciduous forests (hypothetic)	?	cold-temperate	?	?	680	?	?	0.45		*Jarvis and Leverenz* [1983]
Mean									0.74		

Table 2. (continued)

Vegetation Type	Species	Age	Locality	Growing Season	R_0	S_i	P_a	L_{max}	e_a	e	References
AF	fir	4	Japan	?	?	?	840	7.7	0.51		*Kira* [1975]
	fir	25	Japan	?	?	?	1680	9.7	1.31		*Kira* [1975]
	fir	60	Japan	?	?	?	1280	9.2	1.04		*Kira* [1975]
	Scots pine	young	Sweden	?	?	?		1.0	1.42		*Jarvis and Leverenz* [1983]
	Scots pine	14	Sweden	01.05/15.10	3322	830	1250	1.4	1.50		*Ågren et al.*[1979], *Perttu et al.* [1979]
Mean									1.09		
TG	mixed prairie	?	Saskatchewan, Canada	?	?	497	369	0.9	0.74		*Ripley and Saugier* [1975], *Coupland* [1974]
	Solidago altissima	?	Japan	?	?	?	399	5.0	0.98		*Kira et al.* [1969]
	salt marsh	?	United States East Coast	?	?	?	?	?	0.79		*Bartlett et al.* [1990]
Mean									0.84		
EFc	oil palm, no water stress	?	Ivory Coast	12 months	5095	1898	2360	4.5	1.24	1.83	*Dufrêne et al.* [1990]
	oil palm, water stress	?	Ivory Coast	12 months	5095	1898	1940	4.5	1.02	1.60	*Dufrêne et al.* [1990]
	oil palm	?	Indonesia	12 months	5930	2336	2990	5.0	1.28	1.80	*Dufrêne et al.* [1990]
Mean									1.18	1.74	
OFc	pine, fertilized		Florida	12 months	?	1758	1400	?	0.80		*Gholz et al.* [1991]
	pine, control		Florida	12 months	?	?	830	?	0.46		*Gholz et al.* [1991]
Mean									0.63		
MFc	eucalyptus, irrigated, fertilized	?	Portugal	12 months	4880	?	3522	3.8	1.60		*Pereira et al.* [1992]
	eucalyptus, irrigated	?	Portugal	12 months	4880	?	2785	3.0	1.56		*Pereira et al.* [1992]
	eucalyptus, fertilized	?	Portugal	12 months	4880	?	2774	2.8	1.42		*Pereira et al.* [1992]
	eucalyptus, control	?	Portugal	12 months	4880	?	2198	2.3	1.36		
	eucalyptus	2 - 10	Australia	12 months	?	?	?	?	0.90		*Linder* [1985]
Mean									1.37		
TFc	willow, control	?	Scotland	?	?	?	800	?	2.11		*Cannell* [1989]
	willow, irrigated, fertilized	?	Scotland	?	?	?	1000	?	2.94	3.59	*Cannell* [1989]
	willow, irrigated, fertilized	4	Sweden	15.05/15.11	2217	889	1460	5.0	1.66		*Eckersten and Nilsson* [1990]
	willow, irrigated, fertilized	5	Sweden	01.05/15.11	1949	718	1790	6.6	2.48		*Eckersten and Nilsson* [1990]
	willow, irrigated, fertilized	6	Sweden	01.05/15.11	1879	828	1610	5.9	1.93		*Eckersten and Nilsson* [1990]
	poplar, irrigated, fertilized	?	Scotland	?	?	?	500	?	2.11	3.14	*Cannell* [1989]

Table 2. (continued)

Vegetation Type	Species	Age	Locality	Growing Season	R_0	S_i	P_a	L_{max}	e_a	e	References
TFc	poplar, control	2	Belgium	?	?	?	?	?	1.56		*Ceulemans et al.* [1992]
Mean									2.11		
AFc	pine	2 - 12	New Zeland	?	5000	?	?	?	1.34		*Grace et al.* [1987]
	Scots pine, irrigated, fertilized	14	Sweden	?	3322	?	?	?	1.80		*Jarvis and Leverenz* [1983]
	Douglas, fertilized	?	Netherlands	?	3650	1660	2000	?	1.20		F. Mohren (personnal communication, 1991)
	spruce	?	U.S.S.R.	?	4500	?	?	?	0.90		R. Ceulemans (personnal communication, 1991)
Mean									1.31		
	various broadleaved and coniferous plantations	?	various locations	?	?	?	?	?	1.70		*Linder* [1985]
C_3c									2.34		values quoted by
Mean											*Gosse et al.* [1986]
C_4c									2.77		values quoted by
Mean											*Gosse et al.* [1986]

For vegetation types where several values are given by the same author and for the same site, one mean value per author and per site is kept to calculate the mean for the vegetation type. For signification of vegetation-type symbols, see Table 4. A question mark means "unknown information"; R_O, annual incident global radiation (MJ m^{-2} yr^{-1}); S_i, annual absorbed (sometimes intercepted) PAR (MJ m^{-2} yr^{-1}); P_a, annual above-ground dry matter production (g m^{-2} yr^{-1}); L_{max}, maximum leaf area index reached during growing season; e_a, conversion efficiency of absorbed PAR into above-ground dry matter (g MJ^{-1}); e, conversion efficiency into total dry matter (g MJ^{-1}); age, age of vegetation type (years); growing season, duration of growing season (in month), or dates of start and end of growing season (day.month/day.month).

Table 3. Ratios Belowground / Aboveground Net Primary Productivity (P_s/P_a) Found in the literature

Vegetation Type	Species	Locality	P_s/P_a	References
		Natural Vegetation		
EF	rain forest, mature	Malaisia	0.18	*Kira* [1978]
	"	Ivory Coast	0.13	*Müller and Nielson* [1965]
	rain forest , 0 - 20 years	Rio Negro valley	0.08	*Saldarriaga and Luxmoore* [1991]
	rain forest , 20 - 200 years	Rio Negro valley	0.03	*Saldarriaga and Luxmoore* [1991]
Mean			0.11	
OF	dry-deciduous forest	India	0.25	*DeAngelis et al.* [1981]
MF	eucalyptus	Australia	0.17	*DeAngelis et al.* [1981]
TF	beech	Danmark	0.25	*DeAngelis et al.* [1981]
	beech	Germany	0.22	*DeAngelis et al.* [1981]
	beech	Japan	0.15	*DeAngelis et al.* [1981]
	beech	Sweden	0.15	*DeAngelis et al.* [1981]
	Liriodendron	Tennessee	0.95	*DeAngelis et al.* [1981]
	oak / chestnut	Tennessee	0.27	*DeAngelis et al.* [1981]
	broadleaf forest	New Hampshire	0.20	*DeAngelis et al.* [1981]
	oak	Belgium	0.19	*DeAngelis et al.* [1981]
	oak	Wisconsin	0.81	*DeAngelis et al.* [1981]
Mean			0.37	
TF+AF	mixed oak	Poland	0.12	*DeAngelis et al.* [1981]
	mixed oak	Tennessee	0.21	*DeAngelis et al.* [1981]
	mixed oak	Sweden	0.18	*DeAngelis et al.* [1981]
	mixed forest	England	0.27	*DeAngelis et al.* [1981]
	oak / pine	New York	0.39	*Whittaker and Woodwell* [1969]
Mean			0.23	
AF	Scots pine	Sweden	1.70	*Ågren et al.* [1979]
	spruce	Alaska	0.58	*DeAngelis et al.* [1981]
	pine	Tennessee	0.29	*DeAngelis et al.* [1981]
	Pseudotsuga	Oregon	0.62	*DeAngelis et al.* [1981]
	taïga	central forest, U.S.S.R.	0.22	*DeAngelis et al.* [1981]
	taïga	northern U.S.S.R.	0.11	*DeAngelis et al.* [1981]
	taïga	Finland	0.05	*DeAngelis et al.* [1981]
	taïga	Kaselia, U.S.S.R.	0.16	*DeAngelis et al.* [1981]
	subalpine forest	Japan	0.22	*DeAngelis et al.* [1981]
Mean			0.44	
OG	desert grass	U.S. Basin and Range	1.41	*Sims et al.* [1978]
TG	tall grass	U.S. central lowlands	1.58	*Sims et al.* [1978]
	tall grass	Missouri	1.22	*Kucera et al.* [1967]
	mixed grass	U.S. Great Plains	3.00	*Sims et al.* [1978]
	mixed grass	U.S. Great Plains	5.83	*Sims et al.* [1978]
	mixed grass	U.S. Great Plains	2.61	*Sims et al.* [1978]
	short grass	U.S. Great Plains	2.97	*Sims et al.* [1978]
	short grass	U.S. Great Plains	4.36	*Sims et al.* [1978]
	prairie	Saskatchewan, Canada	0.75	*Warembourg* [1982]
Mean			2.78	
AG	alpine prairie	U.S. Rocky Mountains	1.55	*Sims et al.* [1978]
	bog	?	0.59	*Whittaker and Marks* [1975]
	arctic tundra	?	0.77	*Whittaker and Marks* [1975]
Mean			0.97	
		Cultivations		
EFc	oil palm	Ivory Coast	0.47	*Dufrêne et al.* [1990]
	oil palm , water stress	Ivory Coast	0.57	*Dufrêne et al.* [1990]
	oil palm	Indonesia	0.40	*Dufrêne et al.* [1990]
Mean			0.48	
OFc	dry-deciduous	India	0.25	*DeAngelis et al.* [1981]
TFc	poplar	Scotland	0.49	*Cannell* [1989]
	poplar , 7 years	?	0.17	*Whittaker and Marks* [1975]
	willow	Scotland	0.22	*Cannell* [1989]
Mean			0.29	
AFc	pine, 6 years	New Zealand	0.50	*Beets and Pollock* [1987]
	pine , 12 years	New Zealand	0.25	*Beets and Pollock* [1987]
	pine	North Carolina	0.16	*DeAngelis et al.* [1981]
	Douglas	Washington	0.35	*DeAngelis et al.* [1981]

Table 3. (continued)

Vegetation Type	Species	Locality	P_S/P_a	References
	spruce	Sweden	0.19	*DeAngelis et al.* [1981]
	spruce	Scotland	0.32	*Ford* [1982]
Mean			0.29	
TGc	*Dactylis*	France	0.09	*Shakiba* [1983]
	Festuca	France	0.20	*Belanger* [1990]
Mean			0.15	
C_3c	wheat	?	0.21	*Whittaker and Marks* [1975]
	barley	?	0.22	*Whittaker and Marks* [1975]
	sunflower	?	0.09	*Whittaker and Marks* [1975]
C_4c	maize	?	0.05	*Whittaker and Marks* [1975]
Mean (C_3c+C_4c)			0.14	

For signification of vegetation types symbols, see Table 4. Question mark, unknown information.

Table 4. Simplified Vegetation Classification Used for Our Study, and Corresponding *Matthews* [1983] and *Wilson and Henderson-Sellers* [1985] Classes

Symbol	Vegetation Types	Matthews Classes	Wilson Classes
W	water, ice, urban areas	0, 31	0, 1, 3, 80
		Natural Vegetation	
Deserts			
D	desert	30	70
Forests, woodlands, shrublands (F)			
EF	equatorial, tropical, subtropical moist	1, 2, 3	5, 50
OF	tropical, subtropical dry	5, 6, 7, 9, 12, 13, 15, 17, 19	23, 24, 25, 26, 27, 28, 52, 71, 72
MF	Mediterranean evergreen		14, 16, 19
TF	temperate deciduous	4, 11, 16	20, 21
AF	temperate, subpolar, alpine coniferous	8, 14, 18, 20,21	10, 11, 17, 18, 62
Grasslands (G)			
OG	tropical grassland		36
TG	temperate grassland	26, 27, 28, 29	31
AG	tundra, bog	22	2, 61
		Cultivated Vegetation (c)	
C	all cultivations	32	
Tree plantations (Fc)			
EFc	equatorial evergreen		51
OFc	tropical evergreen		
MFc	Mediterranean evergreen		15
TFc	temperate deciduous		22
AFc	temperate, subpolar coniferous		
Herbaceous crops			
C_3c	C_3 nonlegume crop		4, 40, 41, 42, 45, 46, 47, 48, 49
C_4c	C_4 crop		43, 44
TGc	temperate pasture		30
OGc	tropical pasture		33
		Mixed Vegetation	
OG+OF	tropical savanna (tree plus grass)	23, 24, 25	32, 34, 35, 37, 39
TF+AF	temperate mixed (broadleaf plus conifer)	10	12, 13

The symbols are made up of 2 or 3 letters. First letter, latitudinal zone; D, desert; E, equatorial; O,tropical, subtropical; M, Mediterranean; T, temperate; A, Arctic. Second letter, vegetation type; F, forest, woodland, shrubland; G, grassland. Third letter, land-use; no symbol, natural vegetation; c, cultivated.

Table 5. Conversion Efficiencies of Absorbed PAR Into Total Dry Matter for the Major Ecosystem Types, As Calculated From the Literature Data Presented in Tables 2 and 3

Vegetation Type	Mean e_a	Mean P_s/P_a	Mean e
	Mean		
D			1.26 *
EF	0.56	0.11	0.62
OF			0.37 *
MF	0.32	0.17	0.37
TF	0.74	0.37	1.01
AF	1.09	0.44	1.57
TG	0.84	0.5 *	1.26
OG			1.26 *
AG			1.26 *
C	1.67	0.24	2.07
	Minimum		
Vegetation Type	Minimum e_a	Mean P_s/P_a	Minimum e
D			
EF	0.22	0.11	0.24
OF			0.24*
MF			0.24*
TF	0.23	0.37	0.31
AF	0.51	0.44	0.73
TG			0.6 *
OG			0.6 *
AG			0.6 *
C	0.80	0.24	0.99
	Maximum / Mean for Cultivations		
Vegetation Type	Mean e_a	Mean P_s/P_a	Mean e
EFc	1.18	0.48	1.74
OFc	0.63	0.25	0.79 *
MFc	1.37	0.25 *	1.71 *
TFc	2.11	0.29	2.72
AFc	1.31	0.29	1.69
C_3c			2.71
C_4c			3.51

e_a, conversion efficiency of absorbed PAR into aboveground dry matter (g MJ^{-1}); P_s/P_a, ratio underground / aboveground NPP; $e = e_a \times (1 + P_s/P_a)$, conversion efficiency of absorbed PAR into total dry matter (g MJ^{-1}). Bottom table, mean e_a, P_s/P_a and e for cultivation types are assumed to give maximum e for corresponding natural vegetation types. For definition of vegetation type symbols, see Table 4.

* Values determined arbitrarily (see text).

following: (1) Tropical forests have the same e as Mediterranean forests. (2) An arbitrary P_s/P_a ratio of 0.5 is assigned to temperate grasslands. (3) All grasslands (tropical and Arctic) as well as deserts have the same e as temperate grasslands; for tropical grasslands, we consider that the possible increase of e due to a higher fraction in grasses of the C_4 metabolic type is compensated by a reduction due to water limitation. (4) The mean e for all cultivation types (herbaceous and woody crops) is assigned to the Matthews cultivation type. (5) Mixed vegetation types (such as mixed coniferous / broad-leaved forests, or savannas of trees and grasses) have an e that is the mean e of the two types composing the ecosystem, weighted by the respective cover fraction of the two, whenever it is explicit. The top part of Table 5 recapitulates the mean e per biomes used in this experiment.

4.2. Sensitivity Studies

Sensitivity studies consisted in running the model described above with alternative input data sets, and comparing the outputs with those of reference experiment.

4.2.1. Effect of biome-dependent *e*, experiments CST and CST2. *Heimann and Keeling* [1989] used the parametric model described to estimate terrestrial NPP with the following input data: e is constant and equal to 2.98 g dry matter produced per MJ PAR intercepted [*Monteith*, 1977]; there is a linear relationship between f and the simple ratio (SR) of the raw digital counts in the NIR and R channels.

Experiment CST: In experiment CST, the model was run with a constant e of 2.98 g dry matter produced per MJ PAR absorbed and our own linear relationship between f and "surface" NDVI (equation (6)).

Experiment CST2: Experiment CST as well as *Heimann and Keeling* [1989] use an unrealistically high conversion efficiency, especially for natural vegetation types (see Table 2). This results in very high values of NPP. Experiment CST2 uses a constant e for all the vegetation types, which is half the value used by Heimann and Keeling: 1.5 g MJ^{-1}.

4.2.2. Effect of land use, experiment NAT. This experiment results from the consideration that the very high values of e found for cultivations in the temperate zone, with probably no water stress and sufficient mineral nutrition, are unrealistic on a global scale. According to *Esser* [1991], NPP for cultivations is always lower than for natural vegetation, the ratio agricultural / natural NPP reaching 1 only in some temperate European countries. We made the hypothesis that e is equal for agricultural and natural vegetation types, so the resulting e in a land pixel is assumed to be e for the potential natural vegetation of the pixel. The e values assigned to natural vegetation types are identical to experiment REF (Table 5 (top)).

4.2.3. Effect of vegetation map, experiment WIL. The Matthews vegetation map does not allow to exploit the differences in the value of e for the different types of cultivations, as there is only one cultivation class. In this experiment we used Wilson and Henderson-Sellers' map [1985]. It has the advantages to distinguish between several cultivation types (in particular herbaceous crops / tree plantations, C_3/C_4 herbaceous crops) and to classify shrublands and grasslands, not only forests, according to their latitudinal zone. The mean e values per biomes for natural vegetation types are given in Table 5 (top), and for cultivated types in Table 5 (bottom).

4.2.4. Sensitivity study on *e*, experiments MIN and MAX. The conversion efficiency coefficient, e, is highly variable in the literature despite *Monteith*'s [1977] assumption, even within cultivated vegetation types supposed to be in optimal conditions. This parameter thus introduces a great incertitude on NPP estimates, which we quantified by a sensitivity study. For this

Table 6. Recapitulation of Numerical Experiments Realized and Computed Global NPP (in $Gt_C\ yr^{-1}$).

	Material and Methods				
Experiment	Relation *f*/ Remote Sensing Data	Vegetation Map	Calculation of *e*	Global Radiation	NPP
REF	$f = -0.025 + 1.25 \times NDVI$	*Matthews* [1983], natural vegetation and land-use map	mean *e* per vegetation type, Table 5(top); *e* for composite pixels, equation 10	from GCM	59
NAT	$f = -0.025 + 1.25 \times NDVI$	*Matthews* [1983], natural vegetation map	mean *e* per vegetation type, Table 5(middle), natural vegetation only	from GCM	49
WIL	$f = -0.025 + 1.25 \times NDVI$	*Wilson and Henderson-Sellers* [1985], major vegetation map	mean *e* per vegetation type, Table 5(top) (natural), Table 5(bottom) (cultivated type); major vegetation type (over 50% cover fraction)	from GCM	60
CST	$f = -0.025 + 1.25 \times NDVI$	none	*e* constant = 2.98 g MJ^{-1}	from GCM	145
CST2	$f = -0.025 + 1.25 \times NDVI$	none	*e* constant = 1.5 g MJ^{-1}	from GCM	68
MIN	$f = -0.025 + 1.25 \times NDVI$	*Matthews* [1983], natural vegetation and land-use map	minimum *e* per vegetation type, Table 5(middle); *e* for composite pixels, equation 10	from GCM	27
MAX	$f = -0.025 + 1.25 \times NDVI$	*Matthews* [1983], natural vegetation and land-use map	maximum *e* per vegetation type, Table 5(bottom); *e* for composite pixels, equation 10	from GCM	150
SR	$f = -0.115 + 0.11 \times SR$	*Matthews* [1983], natural vegetation and land-use map	mean *e* per vegetation type, Table 5(top); *e* for composite pixels, equation 10	from GCM	20
SAT	$f = -0.025 + 1.25 \times NDVI$	*Matthews* [1983], natural vegetation and land-use map	mean *e* per vegetation type, Table 5(top); *e* for composite pixels, equation 10	from satellite data	61

For experiments REF, SR, SAT, MIN and MAX, calculation of conversion efficiency *e* for composite pixels is as follows: $e = (1-c) \times e(\text{nat}) + c \times e(\text{cult})$ (equation (10)) with *e*, conversion efficieny of the pixel; *c*, fraction of cultivation (from Matthews land-use map); *e*(nat), conversion efficiency of natural vegetation (vegetation type from Matthews potential vegetation type) *e*(cult), mean conversion efficiency of cultivations. For experiment WIL, calculation of conversion efficiency *e* is as follows: $e = e(\text{maj})$ with *e*(maj), *e* for major plant cover type (c>50%, from Wilson and Henderson-Sellers major plant cover map) ($e(\text{maj}) = e(\text{nat})$ if major type is natural or $e(\text{maj}) = e(\text{cult})$ if major type is cultivated). For experiment NAT, conversion efficiency is calculated as follows: $e = e(\text{nat})$ with *e*(nat), conversion efficiency of natural vegetation (vegetation type from Matthews potential vegetation type).

we ran the model with, respectively, minimal and maximal conversion efficiencies for each vegetation class.

Experiment MIN: For classes where enough raw values of e_a exist, we consider the minimal values (e_a) and calculate minimal *e* with the mean P_s/P_a ratio for the class. The different hypotheses to extrapolate a value of *e* for the classes in which not enough or no literature value could be found are: (1) Mediterranean and tropical forests have the same minimal *e* than equatorial forests. (2) All grasslands are assigned an arbitrary minimal *e* of 0.6. (3) Cultivations are assigned the minimum value of all cultivations (in this case a tropical pine plantation). Table 5 (middle) recapitulates the minimum *e* per biomes used in this experiment.

Experiment MAX: For this experiment the following hypothesis was used: *e* for a given vegetation type is the mean value of the "corresponding" cultivated type; for instance, equatorial, tropical, and subtropical evergreen rain forests (class EF) are given the value found for equatorial tree plantations (class EFc), temperate grasslands the value for C_3 crops, and tropical grasslands the value for C_4 crops. Table 5 (bottom) recapitulates the maximum *e* per cultivation types used in this experiment.

4.2.5. Sensitivity Study on the relationship *f*/NDVI, Experiment SR. *Heimann and Keeling* [1989] assumed a linear relationship between *f* and the simple ratio (SR) of the raw digital counts in the NIR and R channels. The relationship *f*/SR is empirically determined using two points: $f_i = 0$ for NDVI values found in the winter months in southern Alaska: 0.025, $f_i = 1$ for the maximum theoretical NDVI predicted by Kubelka-Monk's theory of scattering in a homogeneous medium: 0.65. Looking through the literature on experimental or modeled relationships between *f* and SR and NDVI, respectively, it is unclear wether *f* is best related linearly to SR or NDVI. In this paper we assumed a linear relation between *f* and NDVI, on the grounds that we found more articles in the literature supporting this relationship. However, supposing there is actually a linear relationship with SR, there would be a strong effect on values of global NPP and maybe also on zonal distribution of NPP. Indeed, using the same endpoints but a linear relationship between *f* and SR results in a relationship between *f* and NDVI very far from linearity: see Figure 2. Experiment SR uses a linear relationship between *f* and SR determined using the same endpoints than were used to obtain relation (6):

$$f = -0.115 + 0.11 \times \text{SR} \tag{9}$$

4.2.6. Sensitivity Study on the Solar Radiation, Experiment SAT. The third parameter of *Kumar and*

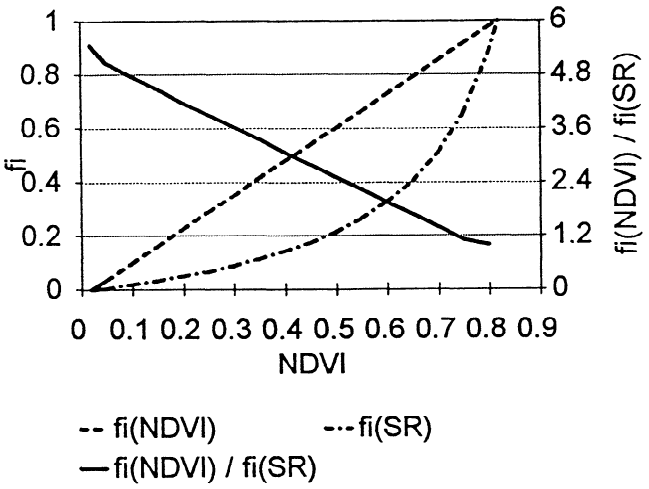

Figure 2. Relationship between interception efficiency of solar radiation, f_i, and NDVI, resulting from linear relationships between f_i and NDVI or SR, respectively. Relationships are determined emipirically using the same endpoints: f_i = 0 corresponds to minimum NDVI = 0.02; f_i = 1 corresponds to maximum NDVI = 0.82 (minimum and maximum of weekly images).

Monteith's [1981] model is incident global radiation. It is obtained in this study using a climatology of monthly solar radiation from a GCM output. Fields of actual solar radiation are not available on a global scale; however we have at our disposition satellite derived solar radiation fieldsl for selected months of years 1985 to 1988 (so called WCRP/GEWEX product) [*Whitlock et al.*, 1993; *DiPasquale and Whitlock*, 1993]. Experiment SAT computes NPP with WCRP/GEWEX solar radiation for January, April, July, and October 1986, resampled on a 1°×1° Plate Carrée projection.

5. Results

In this section we present the results of our reference numerical experiment, concerning global annual NPP, its spatial and its seasonal variations, and compare them with the literature (to convert total dry matter produced into carbon uptake, we used the constant ratio of 0.45 g of carbon in 1 g dry matter [*Ajtay et al.*, 1979]). We also present the results of the sensitivity studies on various parameters.

5.1. Reference Experiment, Experiment REF

5.1.1. Global annual NPP. Table 6 recapitulates the outputs of the various experiments concerning estimated global NPP.

To determine if our global NPP results are realistic, we compare them with global NPP results found in the literature, estimated using different methods: (1) literature data of annual NPP for the major ecosystem types which are compiled and spatially extrapolated using maps of vegetation types; (2) statistical models derived from the Miami model [*Lieth*, 1975]; (3) process models, whenever they compute a global NPP.

Experiment REF results in a global annual NPP estimation of 59 Gt_C. This value is within the intervals of variations in the values estimated by other authors using different methods. Compilation of literature data of annual NPP for the major ecosystem types result in roughly between 40 and 80 Gt_C yr^{-1} for the estimations posterior to 1970 [*Ajtay et al.*, 1979]; more recently, *Fung et al.*'s [1987] estimation is 48 Gt_C. A result of an ecological model of the statistical type is the one of *Box* [1988], who finds 68 Gt_C. A more process-orientated model that can be used as a comparison is the Osnabrück biosphere model (OBM), which results in 36.8 Gt_C yr^{-1} [*Esser*, 1992].

5.1.2. Spatial variations. We illustrate the spatial variations of NPP with maps of annual NPP, the variations of annual NPP averaged over 10° latitude bands with the latitude, and the variations of annual NPP with the vegetation classes.

Productivity maps: The results of the various experiments were used to map annual NPP; experiments REF (with biome-dependent *e*) and CST2 (with constant, "realistic" *e* of half the value used by *Heimann and Keeling* [1989]) are presented in Figure 3 as an example. All the maps constructed from a list of mean conversion efficiencies and a vegetation map have a heterogeneous aspect, due to the discontinuity of the vegetation classification (in reality, there would be, for instance, a continuum of the tree cover fraction from the rain forest to the desert in Africa). However a general tendency is observable and makes our NPP maps with biome-dependent *e* much different than those resulting from statistical ecological models or compilations of literature values (e.g., *Lieth*, 1975) and from the results of *Heimann and Keeling*'s [1989] experiments: higher productivity zones are transferred from the equatorial rain forest regions of the American, African and Asiatic continents to the temperate regions of North America and Europe. This is due mostly to two factors:

1. The calculated values of *e* are lower for equatorial than for temperate forests, probably because they experience a higher mean temperature. On the other hand, they receive a high amount of solar radiation all year-round and their closed canopy enables them to absorb most of it. However, this does not apparently compensate for the negative effect of high temperature.

2. Temperate regions of North America and Europe have a high cultivation fraction (wide regions are 100% cultivated according to the Matthews map), and the calculated *e* for cultivations is very high.

Mean productivity per biome: Table 7 represents the mean, minimal, and maximal annual NPP averaged per biome as computed by experiments REF, MIN, and MAX, compared to the mean, minimal, and maximal literature values given by *Lieth* [1975] which represent well the literature in general. We can note that while all values given by experiment REF are within Lieth's estimates, they are in the lower range for forest types (with differences ranging from about 1:3 to about 1:1 as we go from low- to high-latitude zones), similar for woodlands and shrublands, slightly above the mean for grasslands, and much higher for cultivations (with a difference of 3:1).

On the other hand, experiment CST2 (with *e* constant = 1.5 g MJ^{-1}) results in estimates for annual NPP per biome close to the literature values. If we consider that literature compilations of mean NPP per biomes are representative of the reality, this would lead us to the conclusion that there are no differences of conversion efficiencies between biomes, which were *Monteith*'s [1977] conclusions.

Zonal variations of annual NPP: Figure 4 represents the latitudinal variations of NPP integrated over 10° latitude bands and a year for experiment REF, compared with the outputs of the *Box* [1988] and the OBM model [*Esser*, 1992]. All curves present two peaks, one in the equatorial zone (-10° to 0°) and one in the temperate northern temperate zone (40° to 50°), but there are two distinct patterns. In the Box and OBM results, the

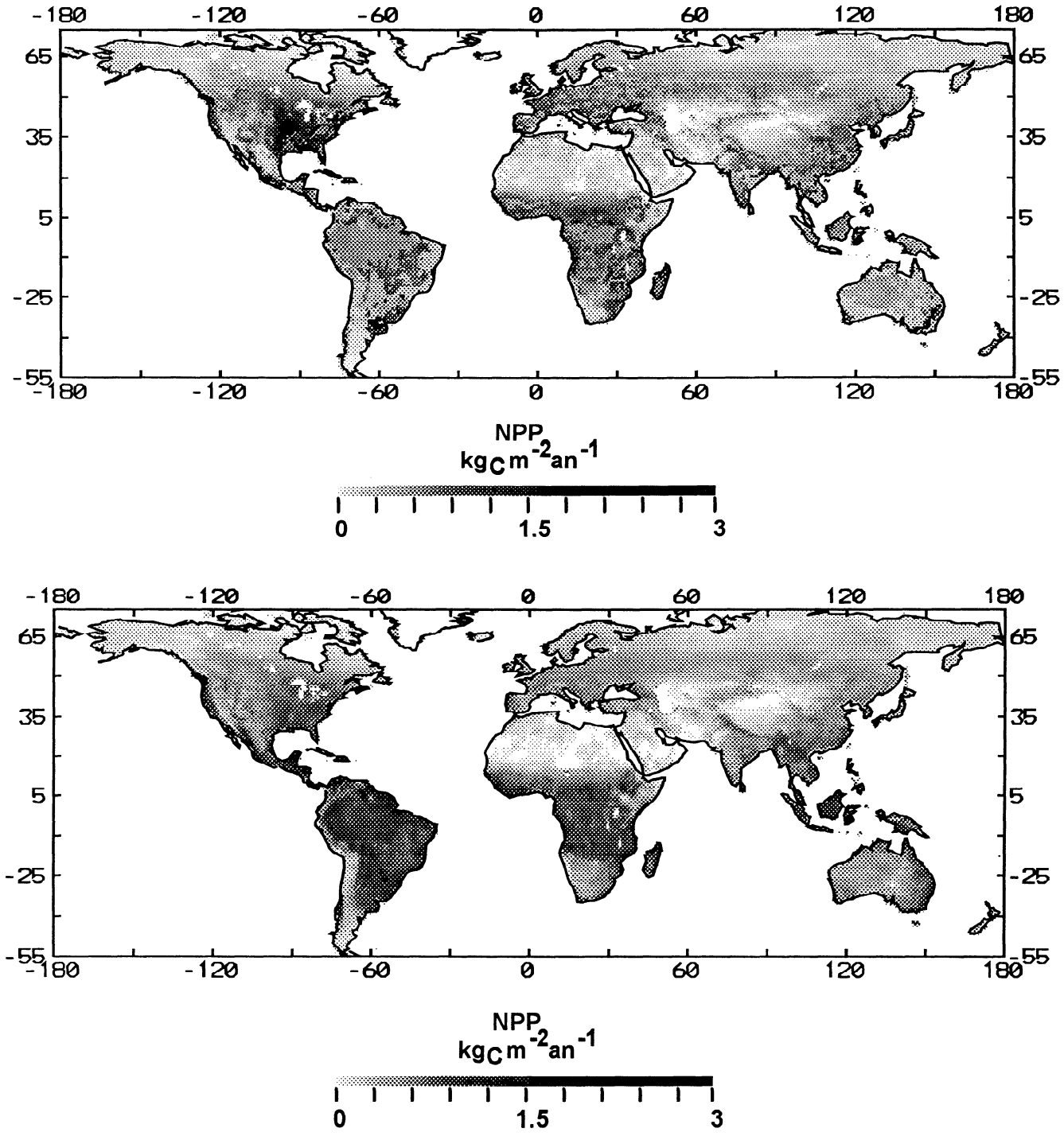

Figure 3. Terrestrial net primary productivity (NPP) maps, as computed by two numerical experiments (see Table 6 for description of the experiments). The maps are in Plate Carrée projection, with a 1°×1° resolution. NPP is integrated over a year. (Top) NPP computed by experiment REF with biome-dependent conversion efficiency *e*. (Bottom) NPP computed by experiment CST2 with constant conversion efficiency *e*.

highest peak is in the equatorial zone while in experiment REF it is located in the temperate latitudes of the northern hemisphere.

In conclusion, while global annual NPP estimated by our experiments are consistent with the literature, our results show much different spatial variations, giving more weight to the northern temperate latitudes (having high cultivation fraction) than to the equatorial latitudes.

5.1.3. Seasonal variations. We illustrate seasonal and spatial variations of NPP with the variations of mean NPP per vegetation class with the season, and the variations of NPP averaged over 10° latitude bands and 4-week periods with the latitude and the season in the form of three-dimensional graphs.

Seasonal variations of NPP per biome: The results from experiment CST2 (with constant *e*) are shown in this section, to compare seasonal variations due to a seasonality in solar

Table 7. Mean, Minimal and Maximal Annual NPP per Vegetation Type (g_C m^{-2} yr^{-1}), and Total Annual NPP for the Biosphere (Gt_C yr^{-1}), As Computed by Experiments REF, MIN and MAX (See Details in Text), and as Given By *Lieth and Whittaker* [1975]

	This Study			*Lieth and Whittaker* [1975]		
Vegetation Type	REF	MIN	MAX	mean	minimum	maximum
			Closed Forests			
equatorial	450	150	2000	1000	450	1600
tropical / Mediterranean	300	100	2000	650	300	1100
temperate / mixed	300	100	900	550	300	1100
boreal	400	100	800	400	200	900
			Woodlands, Schrublands			
all latitudes	180	20	1500	300	100	500
			Grasslands			
savanna	530	200	1700	400	100	700
temperate	470	50	2000	300	100	700
tundra	100	20	300	50	5	200
			Cultivations			
all types	1000	450	1500	300	50	1800
			Total			
	59	27	150	53	22	119

radiation and NDVI only, and not the absolute levels of NPP due to the choice of *e*. Figure 5 represents the seasonal variations of the mean NPP for some of the Matthews vegetation classes. Due to the construction of the Matthews classification, these graphs are not easy to analyze for certain classes in which pixels in much different latitudinal zones are averaged (e.g., some grasslands, cultivations). However, for homogeneous classes, seasonal variations of NPP computed from our experiments are consistent with the known phenology: equatorial rain forests have a relatively constant NPP through the year; both temperate and boreal forests exhibit a peak of activity in summer, because of the limited growing season and the seasonal variations in incoming radiation; temperate grasslands present a reduced but not null activity in the winter.

Seasonal variations of zonal NPP: Figure 6 presents as an example the variations in time and space of NPP integrated over 10° latitude bands and 4-week periods, for experiment REF

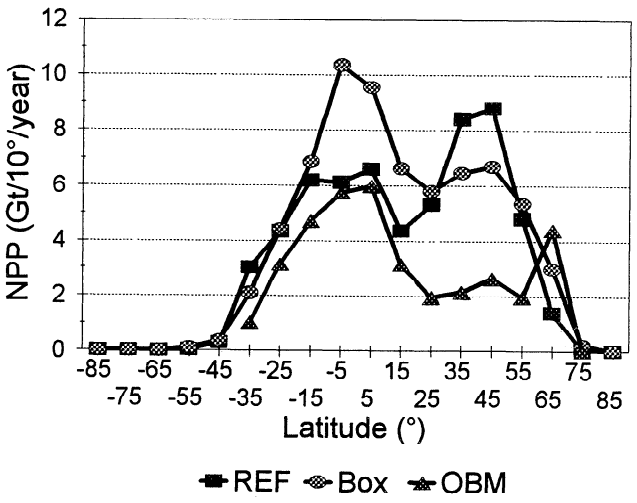

Figure 4. Zonal variations of NPP for reference experiment REF and comparison with literature data: outputs of the statistical model of *Box* [1988], and of the process model "OBM" of *Esser* [1992]. NPP is integrated over a year and 10° latitude bands.

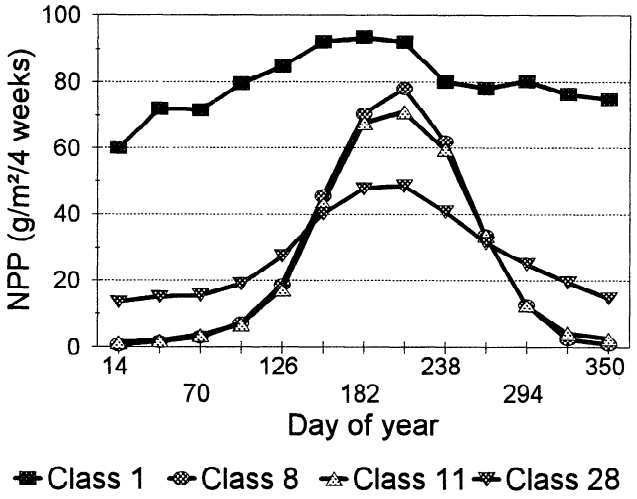

Figure 5. Seasonal variations of mean NPP per vegetation class [*Matthews*, 1983], as computed by numerical experiment CST2 with constant conversion efficiency *e*. NPP is integrated over 4-week periods and averaged for each of Matthews' vegetation classes. The following classes are represented as an example: class 1, tropical / subtropical evergreen rain forest; class 8, subpolar / subalpine evergreen forest; class 11, cold-deciduous forest without evergreens; class 28, short grassland, no woody cover.

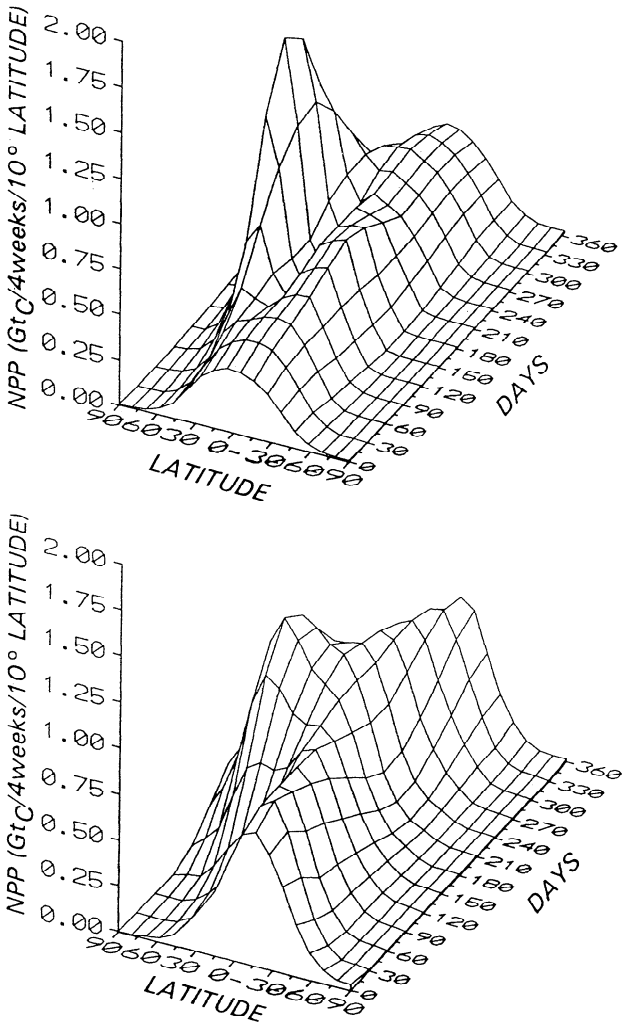

Figure 6. Zonal and seasonal variations of terrestrial NPP as computed by our model, and comparison with literature data. NPP is integrated over 10° latitude bands and 4-week periods. (Top) Zonal and seasonal NPP as computed by experiment REF with biome-dependent *e*. (Bottom) Zonal and seasonal NPP resulting from *Box*'s [1988] ecological model.

(with constant *e*) and according to the *Box* [1988] model. In our results, apart from the already mentioned disproportion between temperate and equatorial zones which is not consistent with the literature, we notice a high summer peak of productivity in the northern hemisphere, but almost no seasonality in the southern hemisphere. This is in contradiction with, e.g., *Box*'s [1988] results, but coherent with the seasonal oscillations of atmospheric CO_2 in the northern hemisphere and the quasi-absence of oscillations in the southern hemisphere [*Keeling et al.*, 1989].

5.2. Sensitivity Studies

The results of all sensitivity studies presented above are illustrated by the latitudinal variations of NPP integrated over 10° latitude bands, and systematically compared to the outputs of reference experiment.

5.2.1. Effect of biome-dependent *e*, experiments CST and CST2. Experiment CST, with an *e* of 2.98 g MJ^{-1}, results in a global NPP of 155 Gt_C yr^{-1}, which is about twice the commonly admitted values. By dividing this value of *e* by 2 (experiment CST2), the estimated productivity is 77 Gt_C, which is within the range of estimation by other authors and in the same order of magnitude as experiment REF. Figure 7a represents the zonal distribution of NPP computed by experiment CST2, compared with the reference REF. The same differences are visible as between REF and the results of the Box and Esser models: the highest peak for CST2 is in the equatorial zone instead of the northern temperate zone for REF.

5.2.2. Effect of land use, experiment NAT. Experiment NAT (with no consideration of a difference in *e* between natural and cultivated vegetation) results in a global NPP reduced by about 20% (49 Gt_C yr^{-1}) compared to experiment REF. Analysis of the zonal variations of NPP (Figure 7b) shows that the largest discrepancies, i.e. the largest ratio NPP(REF) / NPP(NAT), are in the temperate latitudes of the northern hemisphere and the southern hemisphere. In consequence the two peaks of NPP ("northern temperate" and "equatorial") are of the same order of magnitude. This is due to the fact that the zones having the highest cultivation fraction (75% and 100%) on the *Matthews* [1983] land use map, crops being the vegetation type with the highest value of *e*, are concentrated in the eastern half of the United States, western Europe (temperate to Mediterranean northern hemisphere), and, to a lesser extent, India and eastern China (subtropical to tropical northern hemisphere). In the southern hemisphere the few zones with 75% or more of cultivation fraction are less extended again, in Uruguay, southern Africa and the coasts of Australia.

5.2.3. Effect of vegetation map, experiment WIL. Experiments REF and WIL result in an almost identical global annual NPP estimation of about 60 Gt_C, the regional variations of NPP introduced by the differences in conversion efficiency mapping being compensated. Figure 7c represents the zonal variations of NPP with the same model (biome-dependent *e*) and the two different vegetation maps. Roughly, WIL results in "slightly" higher NPP than REF at the northern temperate peak and slightly lower at the equatorial peak. This is due to the fact that the Wilson and Henderson-Sellers map of actual vegetation gives on each pixel the major (over 50% of the surface) plant cover, while Matthews gives rough fractions of natural and cultivated vegetation types (0, 20, 50, 75, and 100%). Therefore in zones with a high cultivation fraction, Wilson and Henderson-Sellers overestimate the cultivation fraction (i.e., our model overestimates *e*), and in in zones with a low cultivation fraction it underestimates it (our model underestimates *e*).

5.2.4. Sensitivity study on *e*, experiments MIN and MAX. The experiments MIN and MAX predict global NPP of 27 and 150 Gt_C yr^{-1}, respectively, i.e. a ratio of nearly 1 to 6, which shows that the incertitude on the estimation of terrestrial NPP with Kumar and Monteith's model is considerable, when no information on the factors influencing *e* is introduced in the model. However, this interval results from extreme hypotheses that are not realistic. Experiment MAX should rather represent the potential terrestrial NPP, that would be attained in non limiting conditions. Figure 7d represents the zonal variations of NPP computed by experiment REF, and of the maximum and minimum NPP computed by experiments MAX and MIN: they give extreme error bars on the estimation of zonal NPP by our model.

5.2.5. Sensitivity study on the relationship *f*/NDVI, experiment SR. Using a linear relationship between *f* and SR (equation 6) results in global NPP nearly 3 times lower than

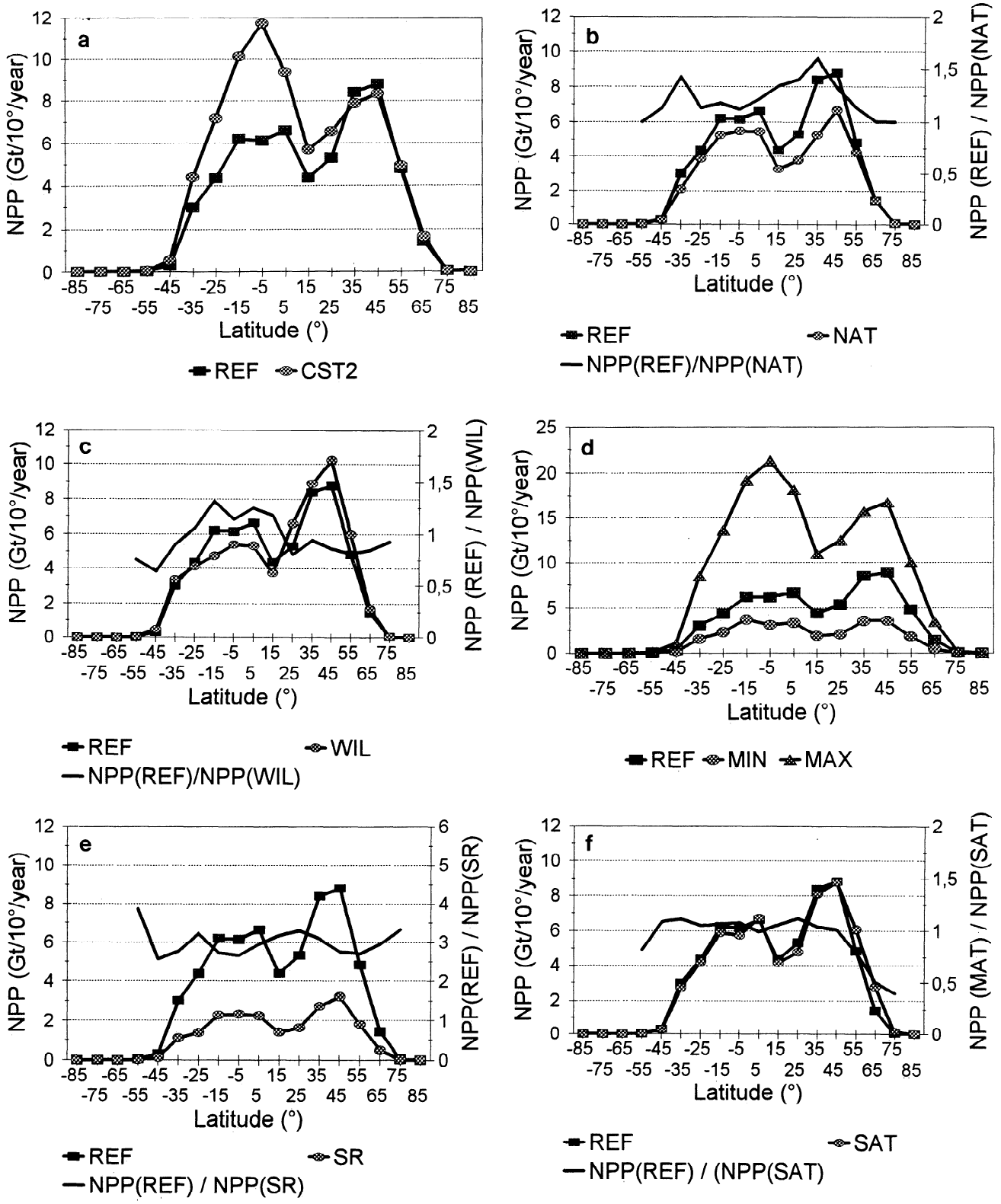

Figure 7. Sensitivity study of various input data on zonal variations of annual NPP. For each experiment, NPP is integrated over 10° latitude bands and a year. (a) Effect of biome-dependent e: experiment CST2 versus experiment REF. (b) Effect of land-use: NPP for experiment NAT versus NPP for experiment REF, and ratio of the two. (c) Sensitivity study on vegetation map: NPP for experiment WIL versus NPP for experiment REF and ratio of the two. (d) Sensitivity study on e: NPP for exp REF, and for experiments MIN and MAX. (e) Sensitivity study on the relationship f/NDVI: NPP for experiment SR versus NPP for experiment REF, and ratio of the two. (f) Sensitivity study on S_0: NPP for experiment SAT versus NPP for experiment REF, and ratio of the two.

REF (20.5 versus 59.4 Gt_C yr^{-1}). Analysis of zonal variations of NPP for the two simulations (Figure 7e) shows a relatively constant ratio of 3 between the two, roughly lower than 3 at the two peaks (zones having mean annual NDVI above the average), and higher than 3 outside the peaks (zones with low mean NDVI).

5.2.6. Sensitivity study on the solar radiation, experiment SAT. There is little difference in the values of monthly global NPP computed by experiment REF and SR. We find, respectively, 3.04 versus 3.16 Gt_C $month^{-1}$ in January, 4.24 versus 4.55 in April, 7.71 versus 7.67 in July, 5.05 versus 4.70 in October. If we multiply by 3 the sum of NPP for the four months computed by experiment SR, we find 60 Gt_C yr^{-1}. Experiment REF results in 59 Gt_C yr^{-1}, which is almost identical. However, there is some systematic differences between the zonal distributions of monthly NPP. Figure 7f represents the zonal distributions of annual NPP computed by experiment REF, the sum of NPP for the four months computed by experiment SR multiplied by 3, and the ratio of the two. This ratio is slightly superior to 1 in all latitude bands, exept for the latitude bands centered above 55° latitude south and north, where it is significantly lower than 1 (as low as about 0.4 for the band centered around 75° north). Indeed, the largest difference between the GCM-derived and the satellite-derived solar radiation is located in boreal, continental zones. There is a significant difference in these zones every month, and it can be as high as 140% for some pixels. However, this is not too sensitive for our NPP model, as the boreal zones do not receive a high amount of solar radiation, and the fraction intercepted is relatively low integrated over a year.

5. Discussion

When we use biome-dependent values of e as inputs for the model, the seasonal and spatial variations of terrestrial NPP are not consistent with the other estimates found in the literature, which also have a high degree of imprecision, although not quantified. There is no evidence to say that the results of a simple statistical model like *Box*'s [1988], for instance, or the compilation of field measurements of NPP [e.g., *Lieth*, 1975] are closer to reality. Because of the very coarse spatial resolution we could not compare our results with local NPP measurements. But we would have other possibilities to validate our results on a global scale, for example, coupling the NPP model with a soil decomposition model (this was done by *Fung et al.* [1987] and *Heimann and Keeling* [1989]), then computing NEP (the net exchanges of CO_2 between the atmosphere and the terrestrial biosphere). These, along with modeled net exchanges between the ocean and the atmosphere, can be integrated in a global circulation model and the results compared with measured atmospheric CO_2 concentration fields. However, the very high imprecision that remains on the model input parameters would have to be corrected before we do any further validation study.

Incoming PAR, S_0: The precision on the incoming global radiation could be improved by using actual solar radiation fields or remote sensing derived solar radiation, for instance, with fine space and time resolution.

Absorption efficiency, f: Satellite data could be further processed to eliminate more atmospheric effects like Mie scattering and compute NDVIs even closer to surface NDVI. However, the main problem is caused by the incertitude on the f/NDVI relationship, which is assumed to be linear and constant in this study. The solution could be to use radiative transfer models of the *Sellers* [1985, 1987] type to model the relationship f/NDVI. It has been done for the African continent by *Leon* [1991], but the availability of input parameters on a global scale is limiting. Another possibility is to classify NDVI time series [*Viovy et al.*, 1992] in order to fix a 0 level of f for each class using the time evolution of the signal.

Conversion efficiency, e: This is the parameter introducing the greatest incertitude on the estimates. The most problematic vegetation types are the ones occupying the widest surface and having the most weight on global NPP and its zonal distribution, i.e., cultivations and equatorial rain forests. For cultivations, most values concerning herbaceous crops were determined from experimental plots in non limiting conditions and can hardly be extrapolated on a global scale. For equatorial rain forests, there is a contrast between *Saldarriaga and Luxmoore*'s [1991] very low values determined precisely and other higher values determined more empirically. To this are added some problems of "minor" importance: the lack of values for some vegetation types such as tropical grasslands and savannas and the heterogeneity of values in the classes where sufficient values were found. One solution may be to model the variations of e with environmental parameters such as water balance (water stresses can lower gross photosynthesis), temperature (on which respiration is highly dependent), and soil nitrogen content (which influences the ratio of belowground to aboveground NPP). Mapping conversion efficiency was also a problem, as we did not find a vegetation map adapted to our problem: *Matthews* [1983] has classes overlapping everal latitude zones and only one cultivation class; *Wilson and Henderson-Sellers* [1985] represent major and secondary vegetation classes but with no information on the proportion of the two. Besides, it would be preferable to exploit the precision we have in space resolution of NDVI and that we could have in the incoming radiation by having a vegetation map with a finer resolution. This is possible by using a vegetation map constructed from NDVI time series classification [*Viovy*, 1990], which would also take into account the interannual variations in vegetation cover.

6. Conclusion

The methodology described in this paper has improved the precision on the estimate of continental net primary productivity (NPP), compared to other studies using *Kumar and Monteith*'s [1981] model for remote sensing of crop growth. This has been done by using more precise input parameters; while an empirical relationship between the efficiency of the absorption of solar radiation by vegetation canopies, f, and a vegetation index, NDVI, is still used, remote sensing data are processed to retrieve a NDVI as close as possible to surface values. A first step toward the introduction of environmental effects on the conversion efficiency of absorbed radiation into organic dry matter, e, has been made, by considering that a mean e per major ecosystem type integrates well the effects of environmental parameters such as mean temperature and water budget as well as interspecies variations. However, because of the lack of data on this parameter for natural vegetation types, especially in the warmer part of the biosphere, a great imprecision remains which in the most extreme hypotheses could result in estimates varying from a factor of 1 to 6. A major improvement could be brought through modeling of e. Additional sensitivity studies show that the model is sensitive to the parametrization of e for each

vegetation class, to the relationship between f and NDVI, but less sensitive to the definition of the vegetation classes, and to the solar radiation.

Our method gave realistic estimates of global annual NPP (60 Gt_C), but zonal NPP variations opposed to the generally admitted results: temperate latitudes of the northern hemisphere have the highest contribution to global NPP in this study. If this result is confirmed, it could significantly modify our knowledge on the global carbon cycle.

Notation

Vegetation-related symbols

NEP	net ecosystem productivity.
NPP	net primary productivity (in text).
P	net primary productivity (in formulae).
P_a	aboveground net primary productivity.
P_s	belowground net primary productivity.
f	"absorption efficiency", fraction of PAR incident absorbed by the canopy.
f_i	"interception efficiency", fraction of PAR incident intercepted by the canopy.
a_{max}	maximum absorption at full light interception.
PAR	photosynthetically active radiation (in text).
S	photosynthetically active radiation (in formulae).
R	global radiation (in formulae): indices for radiation, 0, incident, i, intercepted by the canopy, a, absorbed by the canopy.
e	"conversion efficieny", fraction of absorbed PAR converted into organic dry matter.
e_a	fraction of absorbed PAR converted into aboveground organic dry matter.
L	leaf area index.
k	light extinction coefficient.

Radiative transfer related symbols

ρ_R, ρ_{NIR}	surface reflectances in the red and near-infrared wavelengths, respectively.
ρ_a	atmospheric reflectance.
r	radiance; exponent for reflectances and radiances, (asterisk), top of the atmosphere (TOA).
E_s	solar irradiance in a spectral band.
a	spherical albedo of the atmosphere.
σ_s	solar zenithal angle.
σ_v	observation zenithal angle.
T	transmission in a spectral band.
NDVI	normalized difference vegetation index of red and near-infrared reflectances.
SR	simple ratio of red and near-infrared reflectances.
GVI	global vegetation index

Symbols of numerical simulations

REF	reference experiment
WIL	*Wilson and Henderson-Sellers'* [1989] vegetation map used to map e.
CST	e constant ($e = 2.98$ g MJ^{-1})
CST2	e constant ($e = 1.5$ g MJ^{-1})
MIN	e minimum
MAX	e maximum
SAT	global radiation from satellite-derived data
SR	use of a linear relationship between f and SR

References

Ågren, G.I., B. Axelsson, J.G.K. Flower-Ellis, S. Linder, H. Persson, H. Staaf, and E. Troeng, Annual carbon budget for a young Scots pine, in *Structure and Function of Northern Coniferous Forests*, edited by T. Persson, pp. 307-313, *Ecol. Bull.* 32, 1979.

Ajtay, G.L., P. Ketner, and P. Duvigneaud, Terrestrial primary production and phytomass, in *The Global Carbon Cycle*, edited by B. Bolin, E.T. Degens, S. Kempe, and P. Ketner, pp. 129-182, John Wiley, New York, 1979.

Asrar, G., M. Fuchs, E.T. Kanemasu, and J.L. Hatfield, Estimating absorbed photosynthetically active radiation and leaf area index from spectral reflectance in wheat, *Agron. J., 76*, 300-306, 1984.

Baldocchi, D.D., S.B. Verma, and D.E. Anderson, Canopy photosynthesis and water-use efficiency in a deciduous forest, *J. Appl. Ecol., 24*, 251-260, 1987.

Baret, F, and O. Olioso, Estimation à partir de mesures de réflectance spectrale du rayonnement photosynthétiquement actif absorbé par une culture de blé, *Agronomie, 9*, 885-895, 1989.

Baret, F., G. Guyot, and D.J. Major, Crop biomass evaluation using radiometric measurements, *Photogrammetria (PRS), 43*, 241-256, 1989.

Bartlett, D.S., G.J Whiting., and J.M. Hartmann, Use of vegetation indices to estimate intercepted solar radiation and net carbon dioxide exchange of a grass canopy, *Remote Sens. Environ., 30*, 115-128, 1990.

Beets, P.N., and D.S. Pollock, Accumulation and partitionning of dry matter in *Pinus radiata* as related to stand age and thinning, *N. Z. J. For. Sci., 17*(2/3), 246-271, 1987.

Belanger, G., Incidence de la fertilisation azotée et de la saison sur la croissance, l'assimilation et la répartition du carbone dans un couvert de Fétuque élevée en conditions naturelles, Ph.D. thesis, 167 p., Univ. Paris-Sud, Orsay, 1990.

Bernhart-Reversat, F., G. Lemée, and C. Huttel, La forêt sempervirente de basse Côte-d'Ivoire, in *Problèmes d'Ecologie: Structure et Fonctionnement des Ecosystemes Terrestres*, pp. 313-345, Masson, Paris, 1978.

Box, E.O., Estimating the seasonal carbon source-sink geography of a natural, steady-state terrestrial biosphere, *J. Appl. Meteorol., 27*, 1109-1123, 1988.

Cannell, M.G.R., Light interception, light use efficiency and assimilate partitioning in poplar and willow stands, in *Biomass Production by Fast-Growing Trees*, edited by J.S. Pereira, and J.J. Landsberg, pp. 1-12, Kluwer Academic, Dortrecht, 1989.

Ceulemans, R., I. Impens, F. Mau, P. Van Hecke, and S.G. Chen, Dry mass production and solar radiation conversion efficiency of poplar clones, in *Proceedings of the 6th European Conference on Biomass for Energy, Industry and Environment, Athens, Greece, 22-26 April 1991*, edited by G. Grassi, A. Collina and H. Zibetta, pp. 157-163, Elsevier, New York, 1992.

Coupland, R.T., Producers, VI, Summary of studies of primary production by biomass and shoot observation methods, *Tech. Rep. 62*, 84 pp., Matador project, Univ. of Saskatchewan, Saskatoon, 1974.

Daughtry, C.S.T., Estimating absorbed radiation and phytomass from multispectral reflectance of corn and soybeans, in *Proceedings of IGARSS 1988 Symposium, Edinburgh, Scotland, 13-16 Sept. 1988*, pp. 821-824, Eur. Space Agency, Neuilly, France, 1988.

DeAngelis, D.L., R.H. Gardner, and H.H. Shugart, Productivity of forest ecosystems studied during the IBP: The woodlands data set., in *International Biological Programme 23, Dynamic Properties of Forest Ecosystems*, edited by D.E. Reichle, pp. 573-672, Cambridge University Press, New York, 1981.

Dedieu, G., P.Y. Deschamps, and Y.H. Kerr, Satellite estimation of solar irradiance at the surface of the earth and of surface albedo using a physical model applied to Meteosat data, *J. Clim. Appl. Meteorol., 26*, 79-87, 1987.

DiPasquale, R.C., and C.H. Whitlock, First WCRP long-term satellite estimates of surface solar flux for the globe and selected regions, paper presented at the ERIM/JOANNEUM RESEARCH/CIESN 25th International Symposium on Remote Sensing and Global Environmental Change, Graz, Austria, 4-8 April 1993, 1993.

Dufrêne, E., R. Ochs, and B. Saugier, Oil Palm photosynthesis and productivity linked to climatic factors, *Oleagineux*, *45*(8-9), 353-355, 1990.

Eckardt, F., G. Heim, M. Methy, and R. Sauvezon, Interception de l'énergie rayonnante, échanges gazeux et croissance dans une forêt méditerranéenne à feuillage persistant (*Quercetum ilicis*), *Photosynthetica*, *9*(1), 145-156, 1975.

Eckersten, H., and L.O. Nilsson, Light absorption and willow production in southern Sweden, a case study, in *Proceedings of XIX World Congress, International Union of Forest Organizations, Montreal 1990*, pp. 59-67, IUFRO World Congress Organizing Comittee, Montreal, 1990.

Escartin, J.E., Impact des effets atmosphériques sur l'utilisation thématique de l'indice de végétation, Masters thesis, Univ. Perpignan, Paris VI, and Barcelone, 1990.

Esser, G., Osnabrück Biosphere Model: structure, construction, results, in *Modern Ecology, Basic and Applied Aspects*, edited by G. Esser, and D. Overdieck, pp. 679-709, Elsevier, New York, 1991.

Esser, G., Implications of climate change for production and decomposition in grasslands and coniferous forests, *Ecol. Appl.*, *2*(1), 47-54, 1992.

Ford, E.D., High productivity in a polestage Sitka spruce stand and its relation to canopy structure, *Forestry*, *55*(1), 1-17, 1982.

Fung, I.Y., C.J. Tucker, and K.C. Prentice, Application of advanced very high resolution radiometer to study atmosphere-biosphere exchange of CO_2, *J. Geophys. Res.*, *92*, 2999-3015, 1987.

Fung, I.Y., Analysis of the seasonal and geographical patterns of atmospheric CO_2 distributions with a three-dimensional tracer model. In *The Changing Carbon Cycle-A Global Analysis*, edited by J.R. Trabalka, and D.E. Reichle, pp. 459-473, Springer-Verlag, New York, 1986.

Gallo, K.P., C.S.T. Daughtry, and M.E. Bauer, spectral estimation on absorbed photosynthetically active radiation in corn canopies, *Remote Sens. Environ.*, *17*, 221-232, 1985.

Galoux, A., P. Benecke, G. Gietl, H. Hager, C. Kayser, O. Kiese, K.R. Knoerr, C.E. Murphy, G. Schnock, and T.R. Sinclair, Radiation, heat, water and carbon dioxide balances, in *International Biological Programme, 23, Dynamic Properties of Forest Ecosystems*, edited by D.E. Reichle, pp. 87-204, Cambridge University Press, New York, 1981.

Gholz, H.L., S.A. Vogel, W.P. Cropper, Jr, K. Mckelvey, and K.C. Ewel, Dynamics of canopy structure and light interception in *Pinus Elliottii* stands, North Florida, *Ecol. Monogr.*, *61*(1), 35-51, 1991.

Gosse, G., C. Varlet-Grancher, R. Bonhomme, M. Chartier, J.M. Allirand , and G. Lemaire, Production maximale de matère sèche et rayonnement solaire intercepté par un couvert végétal, *Agronomie*, *6*(1), 47-56, 1986.

Grace, J.C., P.G. Jarvis, and J.M. Norman, Modelling the interception of solar radiant energy in intensively managed stands. *N. Z. J. For. Sci.*, *17*(2/3), 193-209, 1987.

Hatfield, J.L., G. Asrar, and E.T. Kanemasu, Intercepted photosynthetically active radiation estimated by spectral reflectance. *Remote Sens. Environ.*, *14*, 65-75, 1984.

Heimann, M., and C.D. Keeling, A three-dimensional model of atmospheric CO_2 transport based on observed winds, 2, Model description and simulated tracer experiments, in *Aspects of Climate Variability in the Pacific and the Western Americas*, edited by D.H. Peterson, pp. 237-274, *Geophys. Monogr.*, *55*, 1989.

Holben, B.N., Characteristics of maximum-value composite images from temporal AVHRR data, calibration, *Int. J. Remote Sens.*, *11*, 1511-1519, 1986.

Holben, B.N., Y.J. Kaufman, and J.D. Kendall, NOAA-11 AVHRR visible and near-IR inflight calibration. *Int. J. Remote Sens.*, *11*, 1511-1519, 1990.

Huete, A.R., Soil influences in remotely sensed vegetation-canopy spectra, in *Theory and Applications of Optical Remote Sensing*, edited by G. Asrar, pp. 107-140, John Wiley, New York, 1989.

Jarvis, P.G., and J.W. Leverenz, Productivity of temperate, deciduous and evergreen forests, in *Encyclopaedia of Plant Physiology*, new series, vol. 12d., edited by O.L. Lange, P.S. Nobel, C.B. Osmond, and H. Ziegler, pp. 233-280, Springer-Verlag, New York, 1983.

Jordan, C.F., Productivity of a tropical forest and its relation to a world pattern of energy storage. *J. Ecol.*, *59*, 127-142, 1971.

Keeling, C.D., R.B. Bacastow, A.F. Carter, S.C. Piper, T.P. Whorf, M. Heimann, W.G. Mook, and H. Roeloffzen, A three-dimensional model of atmospheric CO_2, *Int. J. Remote Sens.*, *7*, 1417-1434, 1989.

Kira, T., Primary production of forests, in *International Biological Programme, 3, Photosynthesis and Productivity in Different Environments*, edited by J.P. Cooper, pp. 5-40, Cambridge University Press, New York, 1975.

Kira, T., Primary productivity of Pasoh Forest-A synthesis, *Malayan Nat. J.*, *30*(2), 291-297, 1978.

Kira, T., K. Shinozaki, and K. Hozumi, Structure of forest canopies as related to their primary productivity, *Plant and Cell Physiology*, *10*, 129-142, 1969.

Kucera, C.L., R.C. Dahlman, and M.R. Koelling, Total net primary productivity and turnover on an energy basis for tallgrass prairie, *Ecology*, *48*(4), 536-541, 1967.

Kumar, M., and J.L. Monteith, Remote sensing of crop growth, in *Plants and the Daylight Spectrum*, edited by H. Smith, pp. 133-144, Academic, San Diego, Calif., 1981.

Lemée, G., La Hêtraie naturelle de Fontainebleau, in *Problèmes d'Ecologie: Structure et Fonctionnement des Ecosystèmes Terrestres*, pp 75-128, Masson, Paris, 1978.

Leon, V., Estimation de paramètres biophysiques (rayonnement photosynthétiquement actif absorbé, photosynthèse) par télédétection spatiale, étude de faisabilité à l'aide d'un modèle de couvert végétal, applications à des données NOAA/AVHRR, D.E.A. Thesis, 78 p., Ecole Nat. Supérieure d'Agron., Rennes, France, 1991.

Lieth, H., Modeling the primary productivity of the world, in *Primary Productivity of the Biosphere*, edited by H. Lieth, and R.H. Whittaker, pp. 237-263, Springer-Verlag, New York, 1975.

Lieth, H., and R.H. Whittaker, Primary production of the major vegetation units of the world, in *Primary Productivity of the Biosphere*, edited by H. Lieth, and R.H. Whittaker, pp. 204-215, Springer-Verlag, New York, 1975.

Linder, S., Potential and actual production in Australian forest stands, in *Research for Forest Management*, edited by J.J. Landsberg, and W. Parsons, pp 11-35, CSIRO, Melbourne, 1985.

Loudjani, P., Cartographie de la production primaire des zones savanicoles d'Afrique de l'Ouest à partir de données satellitaires, comparaison avec des données de terrain, D.E.A. thesis, 94 p., Univ. Paris Sud, Orsay, 1988.

Lüdeke, M.K.B., et al., The Frankfurt Biosphere Model. A global process orientated model for the seasonal and long-term CO_2 exchange between terrestrial ecosystems and the atmosphere, in press, 1993.

Matthews, E., Global vegetation and land use: New high resolution data bases for climate studies. *J. Clim. Appl. Meteorol.*, *22*, 474-487, 1983.

McCree, K.J., Test of current definitions of photosynthetically active radiation against leaf photosynthesis data, *Agric. Meteorol.*, *10*, 442-453, 1972.

Monsi, M., and T. Saeki, Über den Lichtfaktor in den Pflanzengesllschaften und seine Bedeutung für die Stoffproducktion, *Jpn. J. Bot.*, *14*, 22-52, 1953.

Monteith, J.L., Solar radiation and productivity in tropical ecosystems, *J. Appl. Ecol.*, *9*, 744-766, 1972.

Monteith, J.L., Climate and the efficiency of crop production in Britain, *Philo. Trans. R. Soc. London B*, *281*, 277-294, 1977.

Müller, D., and J. Nielson, Production brute, pertes par respiration et production nette dans la forêt ombrophile tropicale, *Forstl. Forsogsvaes. Dan.*, *29*, 60-160, 1965.

Pereira, J.S., C. Araujo, M. Tome, and H. Pereira, Solar radiation and nitrogen use efficiency in *Eucalyptus globulus*, *Proceedings of the 6th European Conference on Biomass for Energy, Industry and Environment, Athens, Greece, 22-26 April 1991*, edited by G. Grassi, A. Collina and H. Zibetta, pp. 191-195, Elsevier, New York, 1992.

Perttu, K., W. Bischof, H. Grip, P.E. Jansson, A. Lindgren, A. Lindroth , and B. Noren, Micrometeorology and hydrology of Pine forest ecosystems, I, Field studies, in *Structure and Function of Northern Coniferous Forests*, edited by T. Persson, pp 75-122, *Ecol. Bull. 32*, Stockholm, 1979.

Peterson, D.L., and S.W. Running, Applications in forest science and management, in *Theory and Applications of Optical Remote Sensing*, edited by G. Asrar, p. 441, John Wiley, New York, 1989.

Planton, S., M. Déqué, and C. Bellevaux, Validation of an annual cycle simulation with a T42-L20 GCM, *Clim. Dyn.*, *5*, 189-200, 1991.

Prince, S.D., A model of regional primary production for use with coarse resolution satellite data, *Int. J. Remote Sens.*, *12*(6), 1313-1330, 1991.

Rahman, H., and G. Dedieu, SMAC: a simplified method for the atmospheric correction of satellite measurements in the solar spectrum, *Remote Sens. Environ.*, in press, 1994.

Rauner, J.L., Deciduous forests, in *Vegetation and the Atmosphere*, edited by J.L. Monteith, pp. 241-264, Academic, San Diego, Calif., 1976.

Ripley, E.A., and B. Saugier, Energy and mass exchange of a native grassland in Saskatchewan, in *Heat and Mass Transfer in the Biosphere*, edited by D.A. De Vries, and N.H. Afgan, Scripta book, John Wiley, New York, 1975.

Sabatier-Tarrago, C., Production de taillis de Châtaignier (*Castanea sativa* Mill.) en relation avec les caractéristiques stationnelles, Ph.D. thesis, 250 p., Univ. Paris-Sud, Orsay, 1989.

Saldarriaga, J.G., and R.J. Luxmoore, Solar energy conversion efficiencies during succession of a tropical rain forest in Amazonia, *J. Trop. Ecol.*, *7*, 233-242, 1991.

Sellers, P.J., Canopy reflectance, photosynthesis and transpiration, *Int. J. Remote Sens.*, *6*, 1335-1372, 1985.

Sellers, P.J., Canopy reflectance, photosynthesis and transpiration, II, The role of biophysics in the linearity of their interdependence, *Remote Sens. Environ.*, *21*, 143-183, 1987.

Shakiba, M.R., Répartition des assimilats carbonés et production dans un peuplement de *Dactylis glomerata* (L.), PhD thesis, 102 p., Univ. des Sci. et Tech. du Languedoc, Montpellier, France, 1983.

Sims, P.L., J.S. Singh, and K.W. Lauenroth, The structure and function of ten North American grasslands, I, Abiotic and vegetational characteristics, *J. Ecol.*, *66*, 251-285, 1978.

Szeicz, G., Solar radiation for plant growth, *J. Appl. Ecol.*, *11*, 617-637, 1974.

Tanré, D., C. Deroo, P. Duhaut, M. Herman, J.J. Morcrette, J. Perbos, and P.Y. Deschamps, Description of a computer code to simulate the satellite signal in the solar spectrum: the 5S code. *Int. J. Remote Sens.*, *11*, 659-668, 1990.

Tans, P.P., I.Y. Fung, and T. Takashaki, Observational constraints on the global atmospheric CO_2 budget, *Science*, *247*, 1431-1438, 1990.

Tarpley, J.D., S.R. Schneider, and R.L. Money, Global vegetation indices from the NOAA-7 meteorological satellite, *J. Clim. and Appl. Meteorol.*, *23*, 491-494, 1984.

Viovy, N., Etude spatiale de la biosphère terrestre: Intégration de modèles écologiques et de mesures de télédétection, Ph.D. thesis, 116 p., Inst. Nat. Polytech., Toulouse, France, 1990.

Viovy, N., O. Arino, and A.S. Belward, The Best Index Slope Extraction (BISE): a method for reducing noise in NDVI time-series, *Int. J. Remote Sens.*, *13* (8), 1585-1590, 1992.

Warembourg, F.R., Ecosystème prairial, 3.3, Répartition et devenir des assimilats dans les écosystèmes prairiaux, *Acta Oecologica Oecologia Generalis*, *3*(1), 75-90, 1982.

Whitlock, C.H., W.F. Charlock, W.F. Staylor, R.T. Pinker, I. Laszlo, R.C. DiPasquale, and N.A. Ritchey, WCRP surface radiation budget shortwave data product description-version 1.1, *NASA Tech. Mem. 107747*, 1993.

Whitlock, C.H., et al., Comparison of surface radiation budget satellite algorithms for downwelled shortwave irradiance with Wisconsin FIRE/SRB surface-truth data, in *Proceedings of the Seventh Conference on Atmospheric Radiation, July 23-27, 1990. San Fancisco, Calif.*, pp. 237-242, American Meteorological Society, Boston, Mass., 1990.

Whittaker, R.H., and P.L. Marks, Methods of assessing terrestrial productivity, in *Primary Productivity of the Biosphere*, edited by H. Lieth, and R.H. Whittaker, pp. 55-118, Springer-Verlag, New York, 1975.

Whittaker, R.H., and G.M. Woodwell, Structure, production and diversity of the oak-pine forest at Brookhaven, New York, *J. Ecol.*, *57*, 157-174, 1969.

Wilson, M.F., and A. Henderson-Sellers, A global archive of land cover and soils data for use in general circulation models, *J. Clim.*, *5*, 119-143, 1985.

A. Ruimy and B. Saugier, Laboratoire d'Ecologie Végétale, C.N.R.S. URA 1492, Bâtiment 362, Université Paris-Sud, 91405 Orsay Cedex, France. (e-mail: ruimy@psisun.u-psud.fr; saugier@psisun.u-psud.fr)

G. Dedieu, Laboratoire d'Etudes et de Recherches en Télédétection Spatiale, C.N.E.S. - C.N.R.S., 18, avenue Edouard Belin, 31055 Toulouse , France. (e-mail: dedieu@lerts.cnes.fr)

(Received July 29, 1992; revised November 10, 1993; accepted November 10, 1993.)